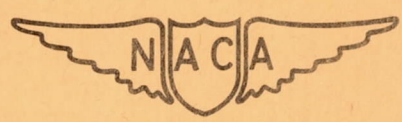# NATIONAL ADVISORY COMMITTEE FOR AERONAUTICS

TECHNICAL NOTE

No. 1511

FLIGHT MEASUREMENTS OF THE LATERAL AND DIRECTIONAL

STABILITY AND CONTROL CHARACTERISTICS OF AN

AIRPLANE HAVING A 35° SWEPTBACK WING WITH

40-PERCENT-SPAN SLOTS AND A COMPARISON

WITH WIND-TUNNEL DATA

By S. A. Sjoberg and J. P. Reeder

Langley Memorial Aeronautical Laboratory
Langley Field, Va.

Washington

January 1948

NATIONAL ADVISORY COMMITTEE FOR AERONAUTICS

TECHNICAL NOTE NO. 1511

FLIGHT MEASUREMENTS OF THE LATERAL AND DIRECTIONAL

STABILITY AND CONTROL CHARACTERISTICS OF AN

AIRPLANE HAVING A 35° SWEPTBACK WING WITH

40-PERCENT-SPAN SLOTS AND A COMPARISON

WITH WIND-TUNNEL DATA

By S. A. Sjoberg and J. P. Reeder

SUMMARY

Flight tests have been conducted to determine the lateral and directional stability and control characteristics of an airplane on which the wing panels are swept back 35°. For these tests, the wings were equipped with slots extending from 40 to 80 percent of the span of the sweptback wing panels measured from the inboard end. Wind-tunnel tests were made of a model of the airplane and wherever possible the flight and wind-tunnel data have been compared.

The directional stability was found to be positive with flaps up or down at all speeds tested. A large increase in dihedral effect with decrease in speed was noted, and the agreement between flight and wind-tunnel measurements of dihedral effect was excellent except at high normal-force coefficients. Oscillations of the airplane and rudder resulting from abrupt deflection and release of the rudder were satisfactorily damped in all cases. The rolling motions involved in the oscillations were greater than normal, however, and the ailerons tended to float in phase with the sideslip angle. Flight and wind-tunnel measurements of the aileron rolling effectiveness expressed by the rate of change of the rolling-moment coefficient with total aileron angle $dC_l/d\delta_a$ were in excellent agreement. The maximum values of the wing-tip helix angle $pb/2V$ reached in rudder fixed aileron rolls were low. At low speed the high dihedral effect caused a considerable reduction in the values of $pb/2V$ that could be obtained.

INTRODUCTION

Flight tests are being conducted at the Langley Laboratory of the NACA to determine the low-speed stability and control characteristics of

an airplane having a 35° sweptback wing. This paper presents the lateral and directional stability and control characteristics with slots along 40 percent of the span of the sweptback wing panels. These slots extended from 40 percent to 80 percent of the span of the sweptback wing panels measured from the inboard end. Wherever possible the flight results are compared with results obtained on a $\frac{1}{4.5}$-scale model of the airplane in the Langley 300 MPH 7- by 10-foot tunnel.

COEFFICIENTS AND SYMBOLS

C_N normal-force coefficient $\left(a_n W/q_c S\right)$

a_n acceleration normal to thrust axis, gravitational units

W airplane weight, pounds

q_c impact pressure, pounds per square foot

S wing area, square feet

δ_a total aileron angle, degrees

δ_r rudder angle, degrees

β sideslip angle, degrees

C_l rolling-moment coefficient $\left(L/q_c Sb\right)$

C_n yawing-moment coefficient $\left(N/q_c Sb\right)$

L rolling moment, foot-pounds

N yawing moment, foot-pounds

b wing span, feet

ψ angle of yaw, degrees

$pb/2V$ wing-tip helix angle, radians

C_{l_p} rate of change of rolling-moment coefficient with wing-tip helix angle $\left(dC_l\middle/d\frac{pb}{2V}\right)$

V true airspeed, feet per second

p rolling velocity, radians per second

AIRPLANE

The airplane tested has the outer wing panels sweptback 35° at the quarter-chord line. A three-view drawing of the test airplane is shown as figure 1 and general dimensions are listed in table I. Figures 2 and 3 are photographs of the airplane. Wing slots which extended from 40 percent to 80 percent of the span of the sweptback wing panels, measured from the inboard end, were installed on the airplane for the present tests. A cross section of the slot and the forward part of the wing in a plane normal to the wing leading edge is shown in figure 4.

The main landing gear of the airplane could not be retracted. The nose gear was retracted for the flap-up tests and extended for the flap-down tests. The variation of aileron position with stick-grip position is shown in figure 5 and the variation of rudder position with rudder-pedal position is shown in figure 6. Because of structural limitations, the airplane was restricted in sideslip. The maximum allowable sideslip angle varied from 15° at 130 miles per hour to 7° at 200 miles per hour.

INSTRUMENTATION

The following instruments were installed in the airplane:

NACA instrument	Measured quantity
Timer	Time (for synchronizing all records)
Airspeed recorder	Airspeed
Control-position recorders	Aileron, rudder, and elevator positions
Control-force recorders	Pedal and stick forces
Sideslip-angle recorder and indicator	Sideslip angle
Recording inclinometer	Angle of bank
Recording accelerometer	Normal, longitudinal, and transverse accelerations
Angular-velocity recorders	Rolling and yawing velocities
Free-air temperature indicator	Temperature

Airspeed was measured with a swiveling static head mounted on a boom
1 chord ahead of the right wing tip and a shielded total head mounted
below the same boom. The airspeed installation was calibrated by means
of a trailing airspeed head. Airspeed as used herein is calibrated
airspeed, which corresponds to the reading of a standard Army—Navy airspeed
meter connected to a pitot—static system free from position error.

Sideslip angles were measured with a vane mounted on a boom 1 chord
ahead of the left wing tip. In order to determine whether angularity of
flow at the wing tip caused errors in the measured sideslip angles, a
calibration flight was made with vanes mounted 1 chord ahead of both
wing tips. The average of the two readings was assumed to be the correct
sideslip angle. These tests showed that the angularity of flow varied
from approximately 0.2° outflow at 110 miles per hour to 1.0° outflow
at 200 miles per hour and that the angularity of flow was independent of
sideslip angle. A correction has been applied to the measured sideslip
angles to account for this effect.

Aileron and rudder positions were measured at the control surfaces,
and the elevator position was measured on the control cable about 8 feet
forward of the elevator.

TESTS, RESULTS, AND DISCUSSION

The lateral and directional stability and control characteristics
were measured in steady sideslips, directional oscillations, rudder kicks,
and aileron rolls. In order to ensure that propeller operation would not
mask any effects of sweepback, all the tests except aileron rolls were
made with the engine idling. Aileron rolls were made with power for
level flight as it expedited the tests, and power effects on the aileron
rolling effectiveness were expected to be negligible.

Steady Sideslips

The static lateral and directional stability and control characteris-
tics as measured in steady sideslips are shown in figure 7 for the flap—up
condition and in figure 8 for the flap—down condition. In the sideslip
at $V_c = 114$ miles per hour (fig. 7(a)), the sideslip—angle range which
could be covered was restricted in a right sideslip both by the available
aileron deflection and wing stalling and in a left sideslip by wing
stalling.

The data show that the rudder—fixed and rudder—free directional
stability, as measured by the variation of rudder angle and rudder force
with sideslip angle, is positive with flaps up or down at all test speeds.

Inspection of the aileron—angle and aileron—force curves of figures 7 and 8 shows a large increase in dihedral effect with decrease in speed.

This increase is shown more clearly in figure 9, where the variation of aileron angle with sideslip angle $d\delta_a/d\beta$ is plotted against normal-force coefficient C_N. The values of $d\delta_a/d\beta$ were measured at zero sideslip angle. The pilot raised mild objections to the high dihedral effect which was present at low speeds because, in making landing approaches and landings, large lateral trim changes accompanied rudder movements. Figure 7(e) shows that the stick—free dihedral effect was negative at the highest speed tested, 198 miles per hour. The pilot objected to this condition, which at higher speed would probably become more pronounced.

Sideslips were also made in the flap—up, engine—idling conditions with the airplane asymmetrically loaded. These flights were made by using gasoline from the nose tank with one wing tank full and the other wing tank empty. This arrangement resulted in rolling moments about the center line of the airplane of approximately ±3200 foot—pounds. This rolling moment is believed accurate to within ±300 foot—pounds. Figure 10 shows the variation of aileron angle with sideslip angle at different speeds with the asymmetric loadings.

In figure 10 at zero sideslip angle, the rolling moment due to the asymmetric load is balanced by the aileron deflections given. Therefore, the variation of rolling—moment coefficient with aileron deflection may be obtained and this variation is shown in figure 11 as the change in rolling—moment coefficient with change in aileron deflection. Figure 11 also includes data obtained in the Langley 300 MPH 7— by 10—foot tunnel on the model of the airplane. The wind—tunnel data presented are for the model with slots along the outer 80 percent of the span of the swept—back wing panels. Some wind—tunnel tests were made without slots on the model. A comparison of these data with those obtained with slots on the model showed that slots had a negligible effect on the aileron effective—ness except at lift coefficients close to the stall. The agreement between the flight data and the wind—tunnel data is excellent.

At the sideslip angles at which the aileron angle is zero in figure 10, the rolling moment due to the asymmetric load is balanced by the rolling moment due to sideslip. The variation of rolling—moment coefficient with sideslip angle was thus obtained for various speeds and these data are presented in figure 12. For convenience in making a comparison with wind—tunnel data, the rolling—moment coefficients have been plotted against yaw angle rather than sideslip angle in figure 12. The yaw angle is numerically equal to the sideslip angle but is of the opposite sign. In figure 13, the variation of $dC_l/d\psi$ with normal—force coefficient as

measured in flight is compared with the wind-tunnel results. Small differences between the flight and tunnel data may be expected from several sources. The wind-tunnel model differed slightly from the airplane in these tests in that on the model the outboard end of the 40-percent slots was at the wing tip and on the airplane the outboard end of the slots was located 20 percent of the span of the sweptback wing panels inboard of the wing tip. The flight values of $dC_l/d\psi$ given in figure 13 cover a considerably larger range of yaw angles than the wind-tunnel values; however, the flight data are nearly linear through zero yaw. In the normal-force-coefficient range in which both flight and wind-tunnel data are available, the agreement is good. No direct comparison of flight and wind-tunnel measurements of dihedral effect and aileron effectiveness are available above a normal-force coefficient of 0.94 since sideslips with the airplane asymmetrically loaded were not made above this normal-force coefficient. The data of figure 9 show that the dihedral effect, as measured by $d\delta_a/d\beta$, is still increasing at a normal-force coefficient of 1.02, but the wind-tunnel data of figure 13 show that the dihedral effect is decreasing above a normal-force coefficient of approximately 0.97. Since the data were obtained near the maximum normal-force coefficient of approximately 1.10, a decrease in aileron effectiveness may have occurred because of stalling. This decrease could account for the tendency of the value of $d\delta_a/d\beta$ to increase in the flight tests. Tuft pictures indicate that the flow over the ailerons was quite unsteady near the stall. Also, the decrease in dihedral effect at high normal-force coefficients shown by the wind-tunnel measurements may be due to the relatively low Reynolds number at which the data were obtained.

Dynamic Directional Stability

The dynamic directional stability characteristics were investigated by abruptly deflecting and releasing the rudder and recording the resulting oscillation. Time histories of these maneuvers using both left and right rudder deflections are shown in figures 14 and 15 for the flap-up, engine-idling condition and in figure 16 for the flap-down, engine-idling condition. In the oscillations at approximately 120 miles per hour (fig. 14) the pilot attempted to hold the stick fixed because insufficient elevator trim tab was available to trim the elevator stick force to zero. In the oscillations at approximately 130 miles per hour (fig. 16) the elevator stick force could still not be trimmed to zero, but in this case the pilot attempted to hold the elevator fixed while not resisting the motion of the ailerons. The oscillations at approximately 200 miles per hour were made with the stick free.

Oscillations of both the rudder and the airplane were satisfactorily damped. The rolling motions associated with the oscillations were relatively large. The ailerons, when free (figs. 15 and 16), oscillated

for several cycles. The pilot objected to the stick "pumping" when he attempted to hold the stick fixed (fig. 14). The data indicate that the ailerons tended to float in phase with the sideslip angle and the aileron oscillation is not attributable to the rolling of the airplane.

Wind-tunnel measurements of the directional stability gave a value of $dC_n/d\beta$ of 0.002 in the flap-up, engine-idling condition. This directional stability is of a magnitude that could be obtained on jet-propelled sweptback-wing airplanes without using such an unusually large vertical tail as that on the test airplane, because the destabilizing effect of the propeller would not be present.

Rudder Kicks

Rudder kicks were made at 120, 135, 160, and 200 miles per hour in the flap-up, engine-idling condition and at 110, 130, and 160 miles per hour in the flap-down, engine-idling condition. In these maneuvers the pilot abruptly deflected the rudder and held it fixed in the deflected position while attempting to hold the control stick fixed. Typical time histories of these maneuvers are presented in figures 17 and 18 for the flap-up, engine-idling condition and in figure 19 for the flap-down, engine-idling condition. The maximum sideslip angle, rolling velocity, yawing velocity, and rudder force obtained are plotted as a function of rudder deflection in figures 20 and 21. In the low-speed tests the airplane turned into a spiral very rapidly and in these cases the maximum yawing velocity used is the first maximum that occurred. The data show that at low speed where the dihedral effect is high the rudder is very effective in producing roll; but, as with straight wings, there is an appreciable lag between the time of application of rudder and the time that maximum rolling velocity is reached.

Aileron Rolls

Rudder-fixed aileron rolls were made at various speeds using power for level flight with the flaps up and down. Typical time histories of left and right aileron rolls made at 150 miles per hour with the flaps up are shown in figure 22. The aileron-roll data were evaluated to determine the variation of aileron effectiveness $pb/2V$ and aileron stick force with aileron deflection. The data for the flap-up condition are shown in figure 23 and for the flap-down condition in figure 24.

At 200 miles per hour with the flaps up, 30° of aileron deflection resulted in a value of $pb/2V$ of 0.052 in a right roll and 0.059 in a left roll. At lower speeds the values of $pb/2V$ were even smaller. The flight values of $pb/2V$ are considerably lower than those estimated

by using the relation $\dfrac{\frac{dC_l}{d\delta_a}\delta_a}{C_{l_p}} = \dfrac{pb}{2V}$ and by neglecting the reduction

in $pb/2V$ resulting from dihedral effect and wing twist. A value of
$dC_l/d\delta_a$ of 0.00096 was obtained from figure 11. A value of C_{l_p} of -0.38
was determined by obtaining from reference 1 the value of C_{l_p} for the
straight wing resulting from unsweeping the sweptback wing and multiplying
this value by the cosine of the sweepback angle. A comparison of values
of C_{l_p} obtained in wind-tunnel tests with values of C_{l_p} found by the
preceding method show good agreement up to sweepback angles of at least 35°.
For 30° of aileron deflection $pb/2V$ was calculated to be 0.076, with no
correction for the effects of sideslip or wing twist.

A brief analysis showed that in flight the rolling moment due to
dihedral effect caused a marked reduction in $pb/2V$. The reduction
in $pb/2V$ was largest at low speeds because of the higher dihedral
effect and larger sideslip angles reached in rolls at low speeds. The
wing of the test airplane had relatively low torsional stiffness; therefore,
even at the moderate and low speeds tested, wing twist may have caused
some reduction in $pb/2V$.

CONCLUSIONS

The conclusions reached concerning the lateral and directional
stability and control characteristics of an airplane having a 35° sweptback
wing with 40-percent-span slots may be summarized as follows:

1. Both the rudder-free and rudder-fixed directional stability were
positive with flaps up or down at all speeds tested.

2. The dihedral effect as measured by the rate of change of
rolling-moment coefficient with angle of yaw $dC_l/d\psi$ increased from
0.0005 at a normal-force coefficient of 0.33 to 0.0025 at a normal-force
coefficient of 0.94. The agreement between the flight and wind-tunnel
measurements of dihedral effect was excellent up to a normal-force
coefficient of approximately 0.97. Above a normal-force coefficient
of 0.97, the wind-tunnel measurements showed $dC_l/d\psi$ decreasing. This
decrease may have been due to the relatively low Reynolds number at
which these tunnel data were obtained. Direct flight measurements
of $dC_l/d\psi$ were not made above a normal-force coefficient of 0.94, but
the flight value of $d\delta_a/d\beta$ (rate of change of total aileron angle with
sideslip angle) continued to increase and indicated that $dC_l/d\psi$ was
still increasing. A part of the increase in $d\delta_a/d\beta$ may have been due
to a loss in aileron effectiveness near the stall.

3. Oscillations of the airplane and rudder produced by abruptly deflecting and releasing the rudder were satisfactorily damped in all cases. The rolling motions involved in the oscillations were greater than normal, however, and the ailerons tended to float in phase with the sideslip angle.

4. Flight measurements of the rolling moment due to aileron deflection gave a value of $dC_l/d\delta_a$ of 0.00096. The wind-tunnel measurements of aileron effectiveness were in excellent agreement with the flight measurements.

5. The maximum values of wing-tip helix angle $pb/2V$ reached in rudder-fixed aileron rolls were low. At 200 miles per hour, deflecting the ailerons a total of 30° resulted in a value of $pb/2V$ of 0.059 in a left roll and 0.052 in a right roll. At lower speeds the values of $pb/2V$ were even smaller. At low speed the dihedral effect caused a marked reduction in the values of $pb/2V$.

Langley Memorial Aeronautical Laboratory
    National Advisory Committee for Aeronautics
        Langley Field, Va., October 15, 1947

REFERENCE

1. Pearson, Henry A., and Jones, Robert T.: Theoretical Stability and
    Control Characteristics of Wings with Various Amounts of Taper
    and Twist. NACA Rep. No. 635, 1938.

TABLE I

AIRPLANE DIMENSIONS AND CHARACTERISTICS

Engine . . . . Allison V-1710

Propeller:
   Diameter, ft 10.375
   Number of blades 3
   Engine - propeller gear ratio 2.23

Normal gross weight, lb. 8700

Wing:
   Span, ft 33.6
   Area, sq ft 250
   Airfoil section (normal to wing leading edge)
     Root . . . . Modified 66,2x-116 (a=0.6)
     Tip . . . . Modified 66,2x-216 (a=0.6)
   Mean aerodynamic chord, in. 93.6
   Leading edge M.A.C.
     (in. behind L.E. root chord) 39.3
   Aspect ratio 4.51
   Taper ratio 1.84:1.00
   Dihedral, deg 0
   Sweepback (25-percent-chord line), deg 35

Plain sealed wing flaps:
   Total area, sq ft 12.52
   Span (along hinge line, each), in. 77.4
   Travel, deg 45

Ailerons:
   Span (along hinge line, each), in. 105
   Area rearward of hinge center line, each, sq ft 6.51
   Travel, deg . . . . ±17

Horizontal tail:
   Span, in. 175
   Total area, sq ft 46.6
   Stabilizer area (including elevator balance), sq ft 37.0
   Elevator area (behind hinge line), sq ft 9.6
   Distance elevator hinge line to L.E. of M.A.C., in. 240.9
   Elevator travel, deg
     Upward 35
     Downward 15

Vertical tail:
   Fixed surface area (above horizontal tail,
     including rudder balance), sq ft 15.5
   Rudder area (behind hinge line), sq ft 8.3
   Total area, sq ft 23.8
   Height along hinge line, in. 78.87
   Distance elevator hinge line to L.E. of M.A.C., in. 263
   Rudder travel, deg . . . . ±30
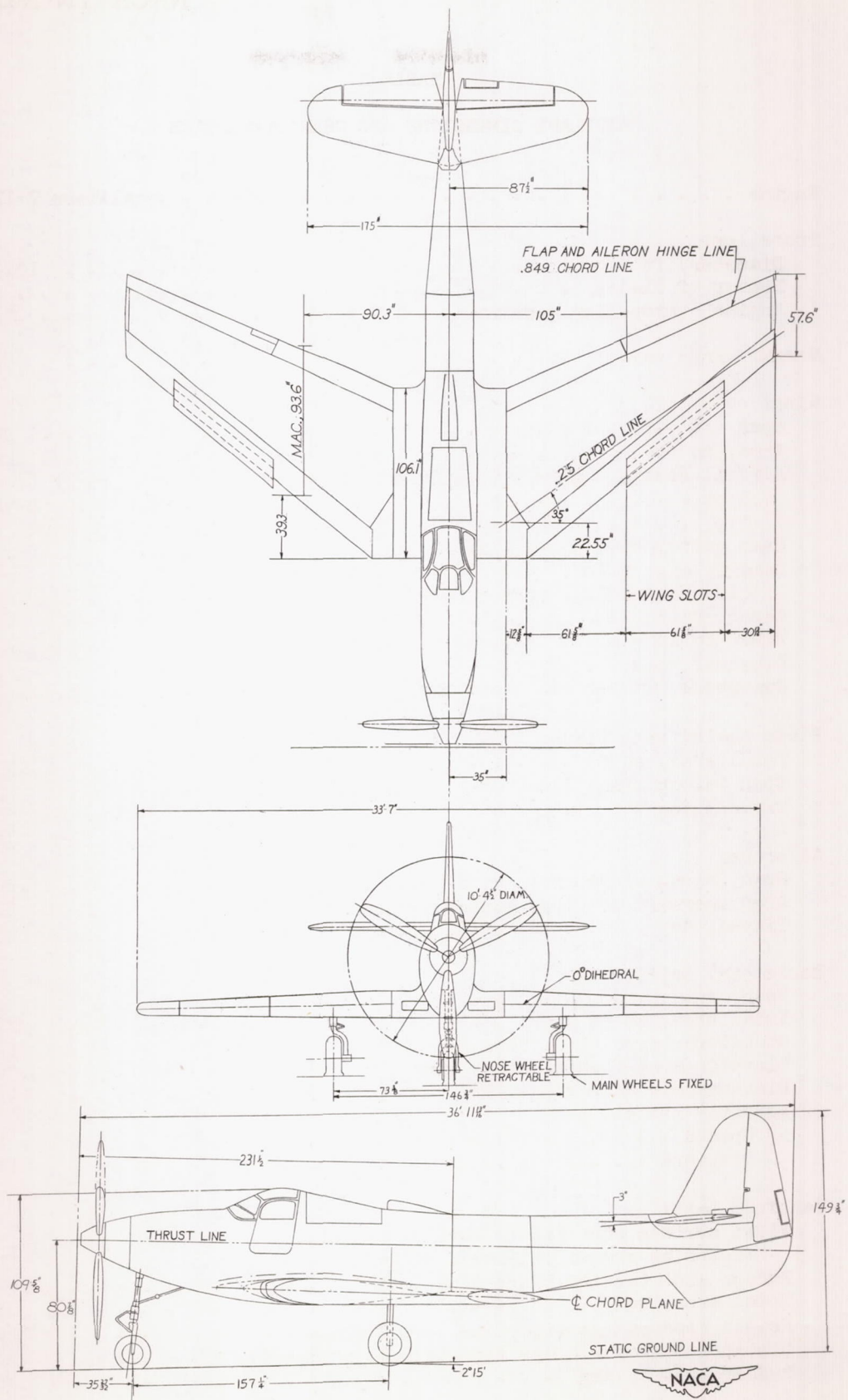
Figure 1.- Three-view drawing of test airplane.
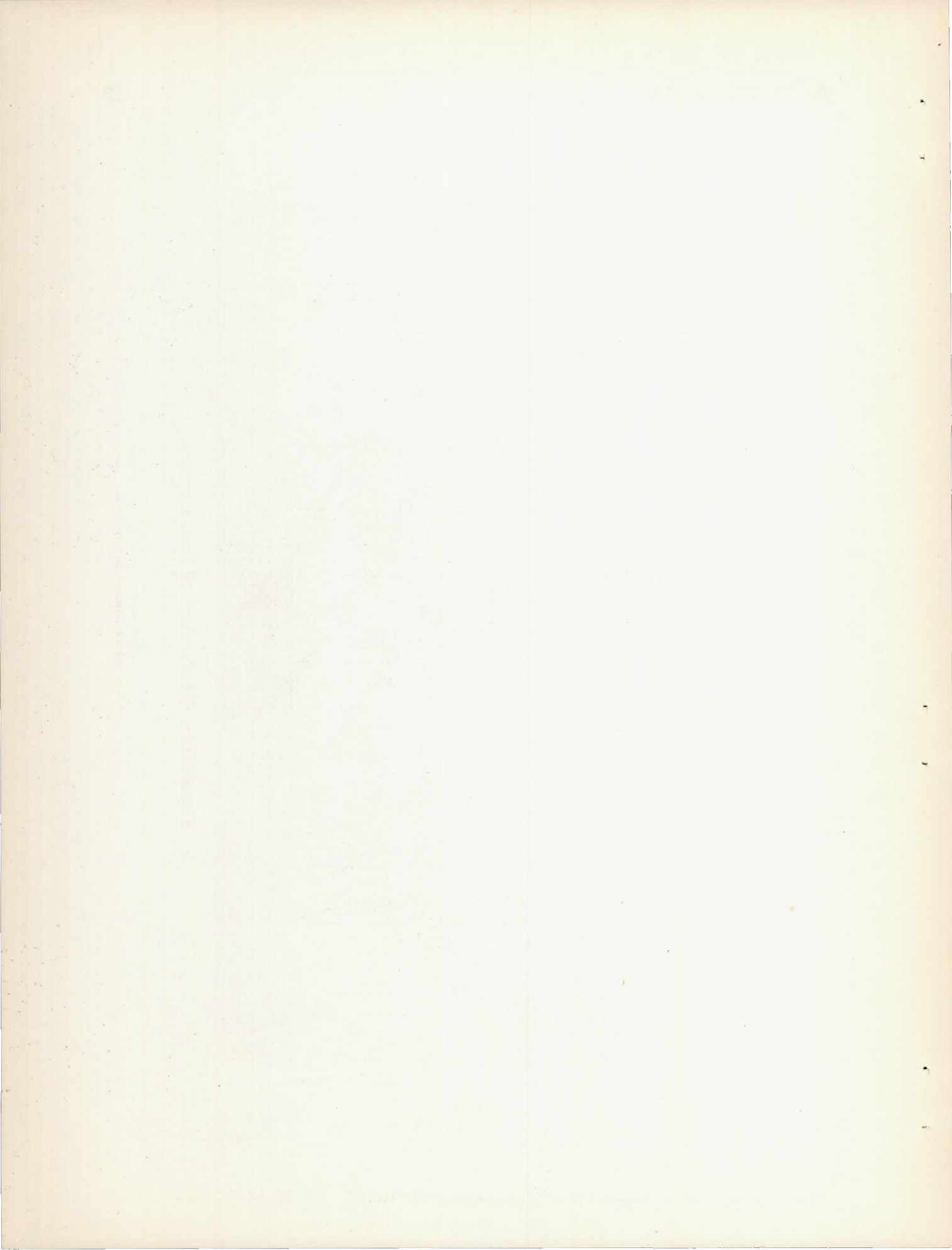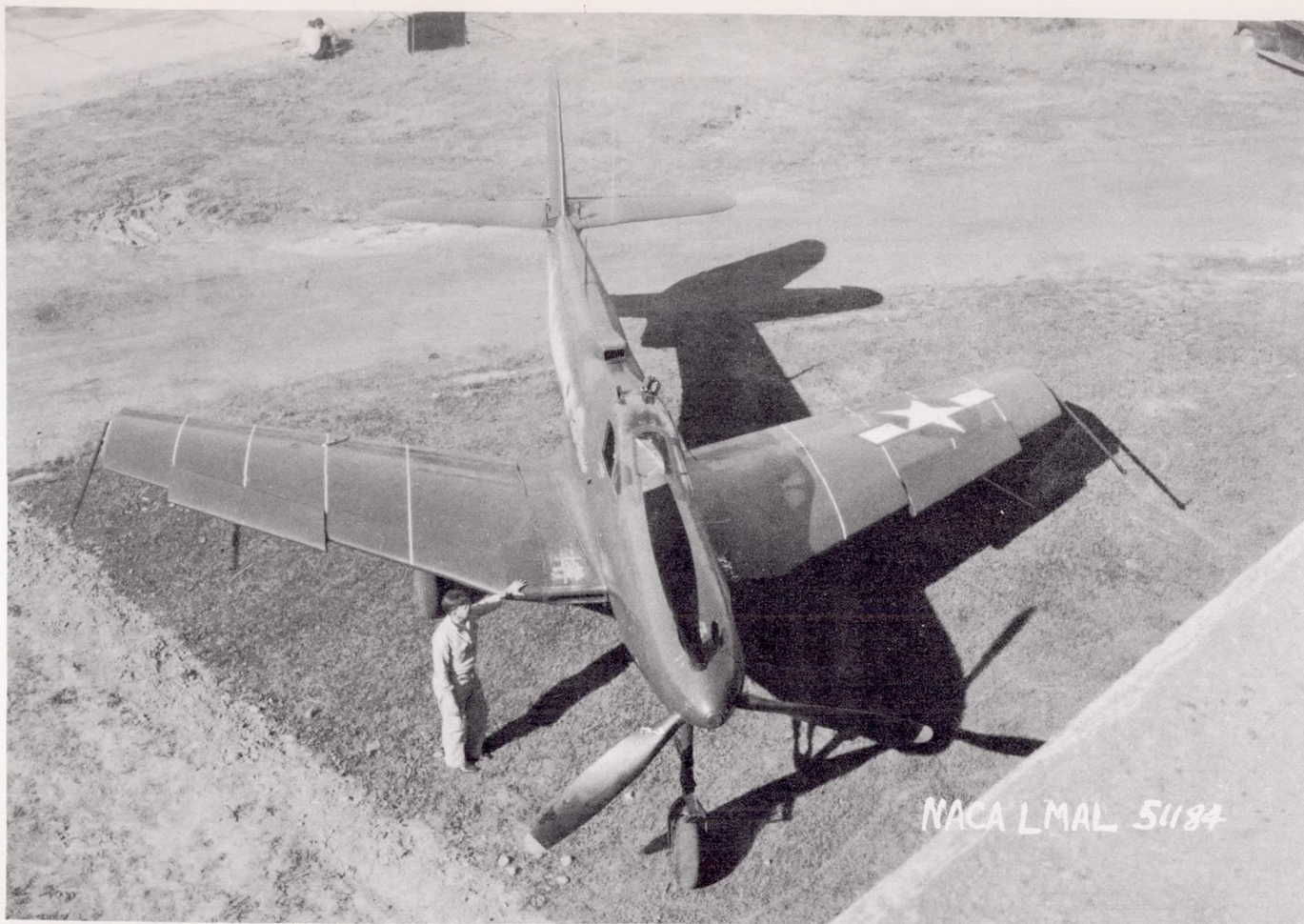
Figure 2.- Front view of test airplane.

NATIONAL ADVISORY COMMITTEE FOR AERONAUTICS
LANGLEY MEMORIAL AERONAUTICAL LABORATORY — LANGLEY FIELD. VA.

NACA LMAL 51186
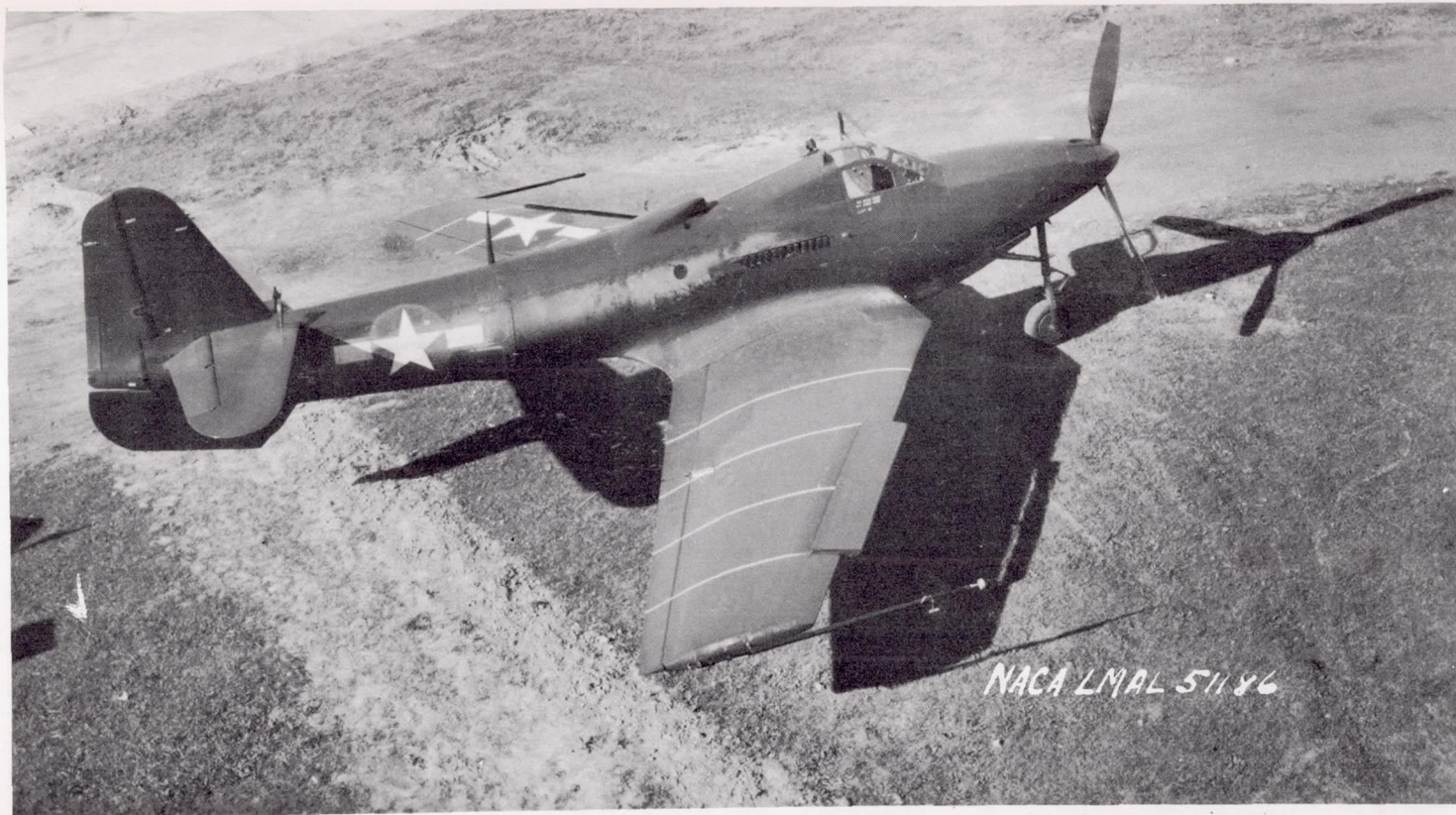
Figure 3.- Side view of test airplane.

NATIONAL ADVISORY COMMITTEE FOR AERONAUTICS
LANGLEY MEMORIAL AERONAUTICAL LABORATORY — LANGLEY FIELD. VA.
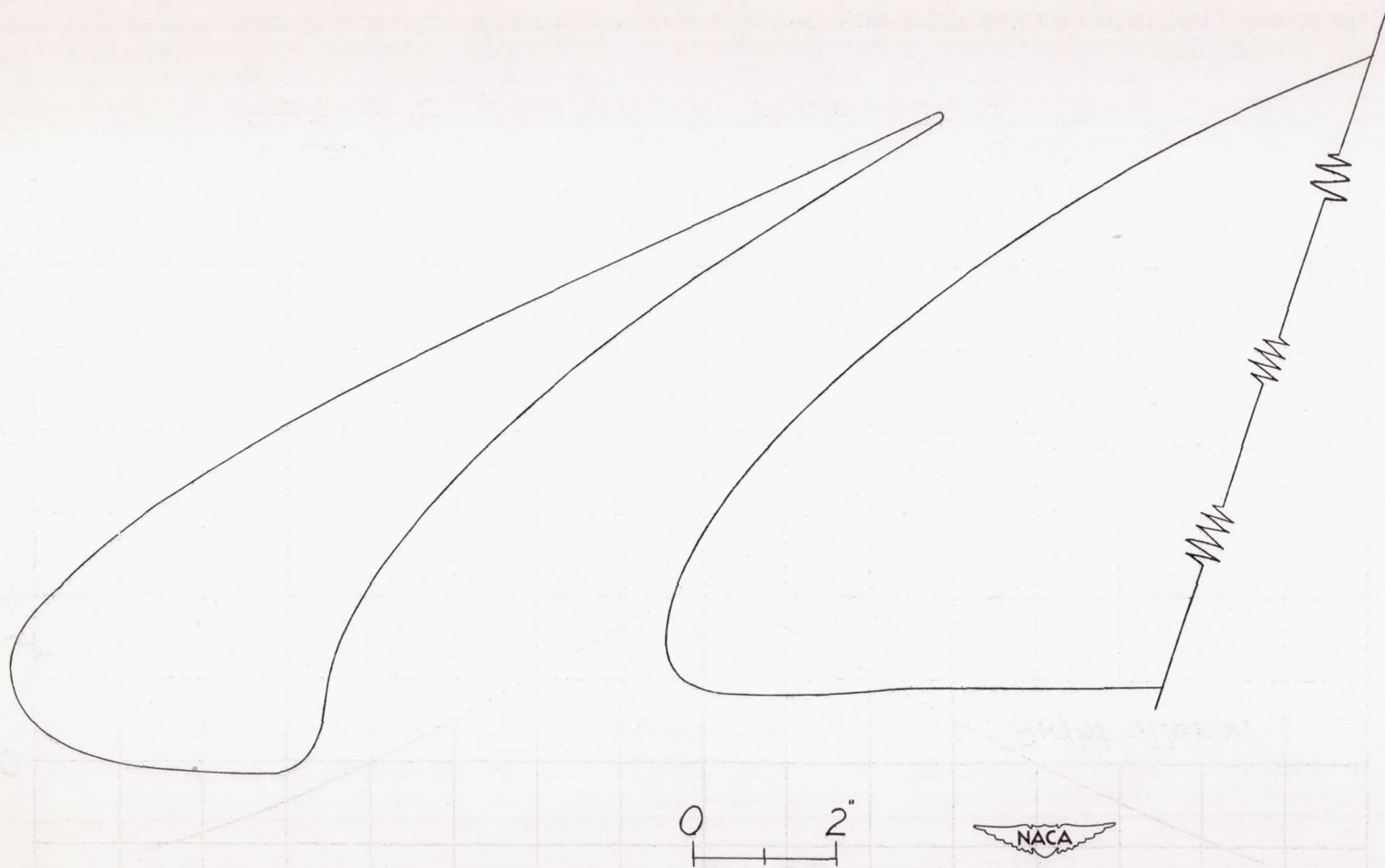
Figure 4.- Section of slot and forward part of wing in plane normal to wing leading edge.
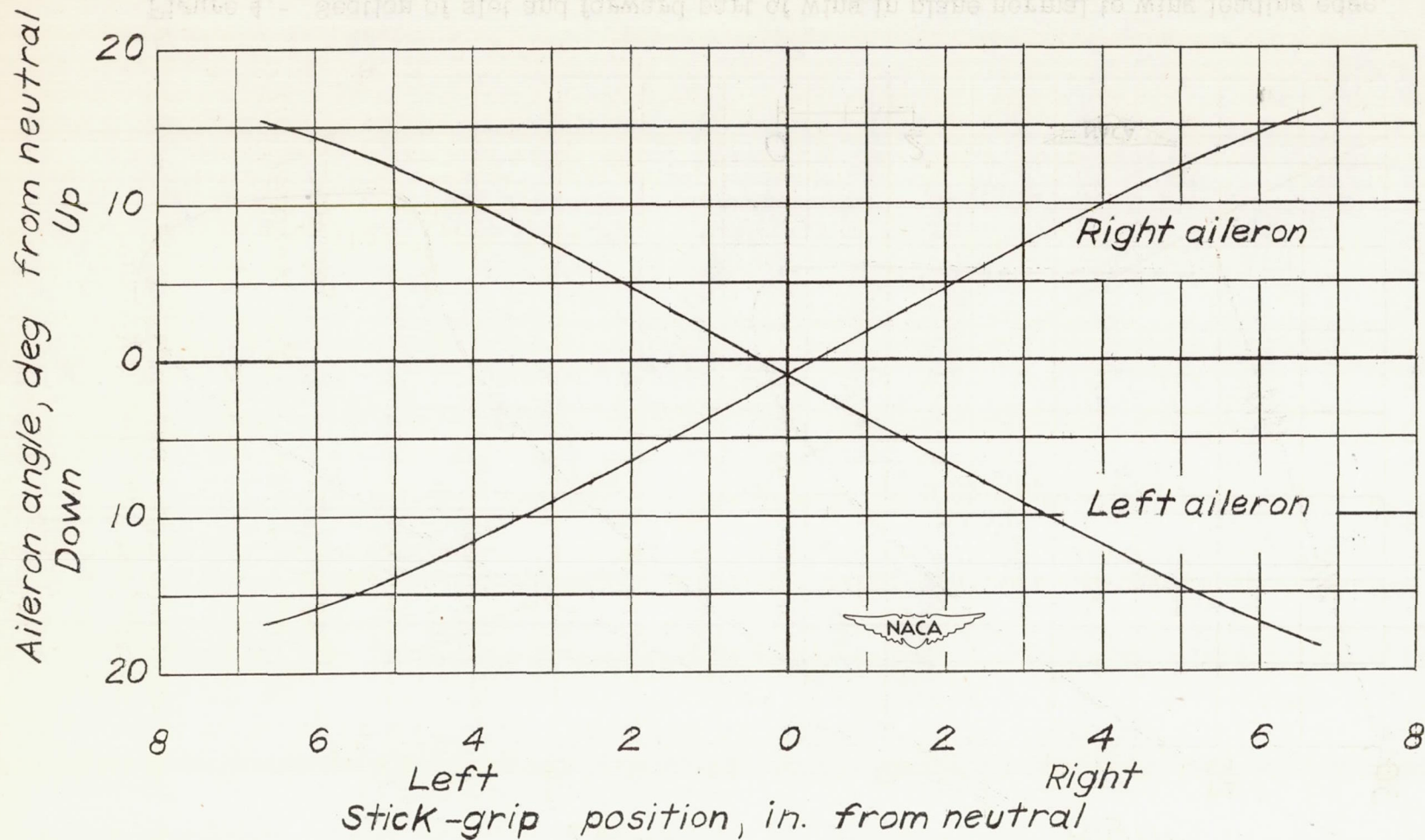
Figure 5.- Variation of stick-grip position with left and right aileron position. No load on system.
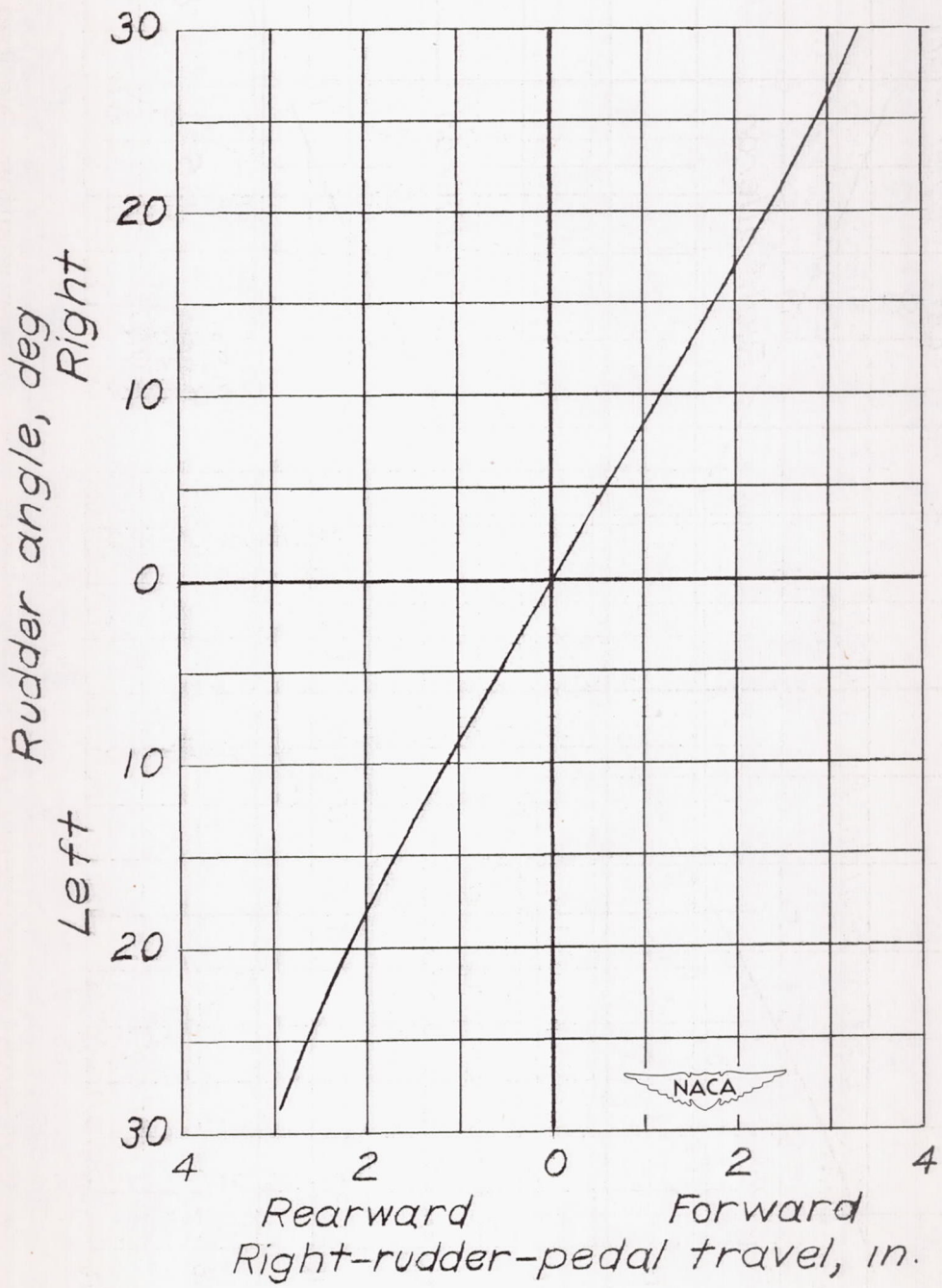
Figure 6.- Variation of right-rudder-pedal position with rudder
position. No load on system.
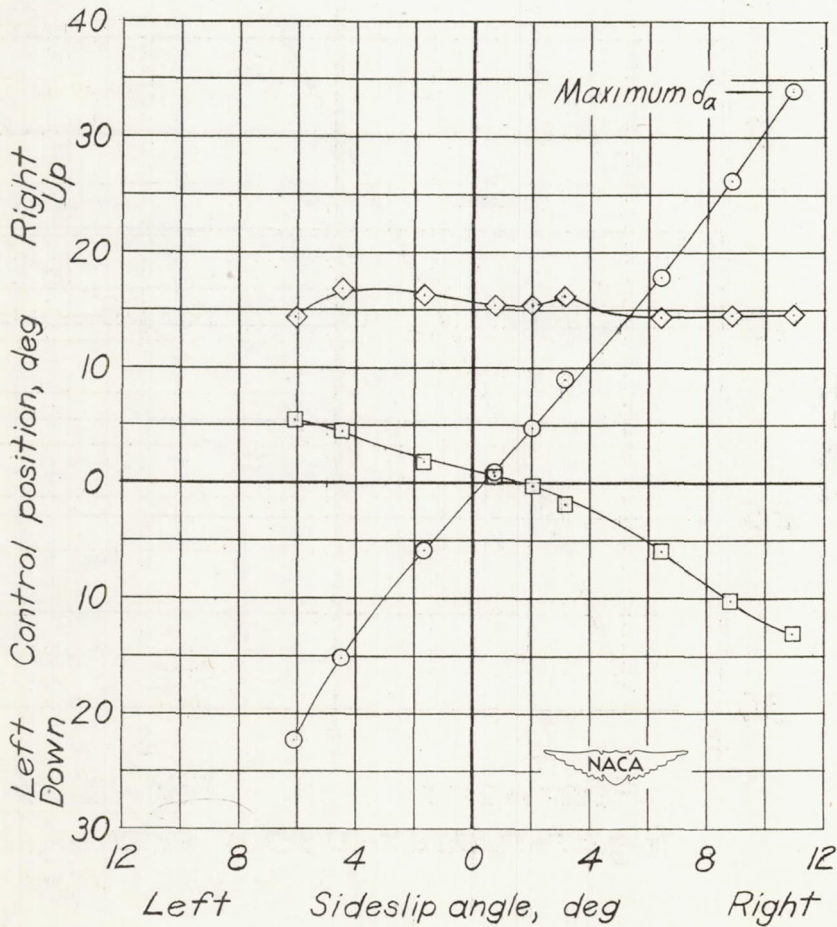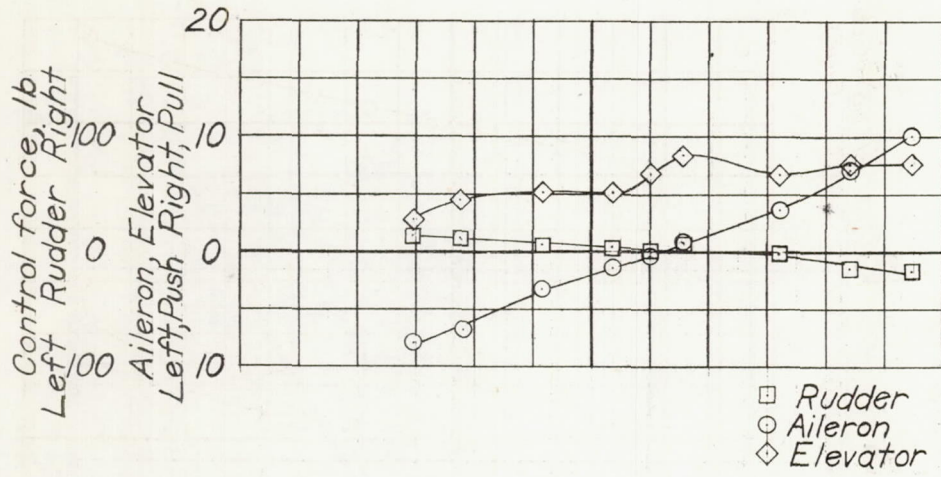
(a) V_c = 114 miles per hour; C_N = 1.02.

Figure 7.- Steady sideslip characteristics with engine idling, flaps up,
nose wheel up.
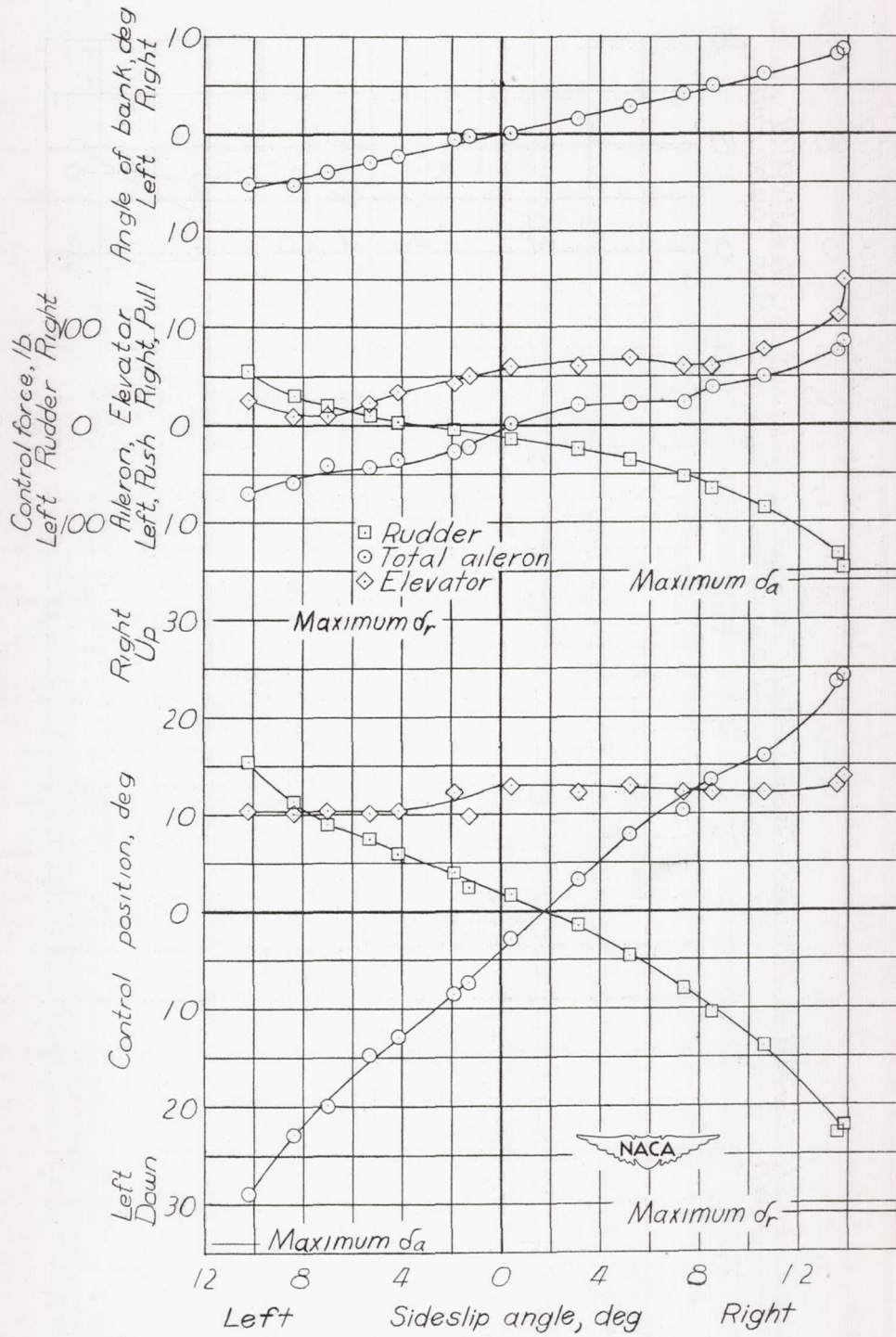
(b) V_c = 119 miles per hour; C_N = 0.96.

Figure 7.- Continued.
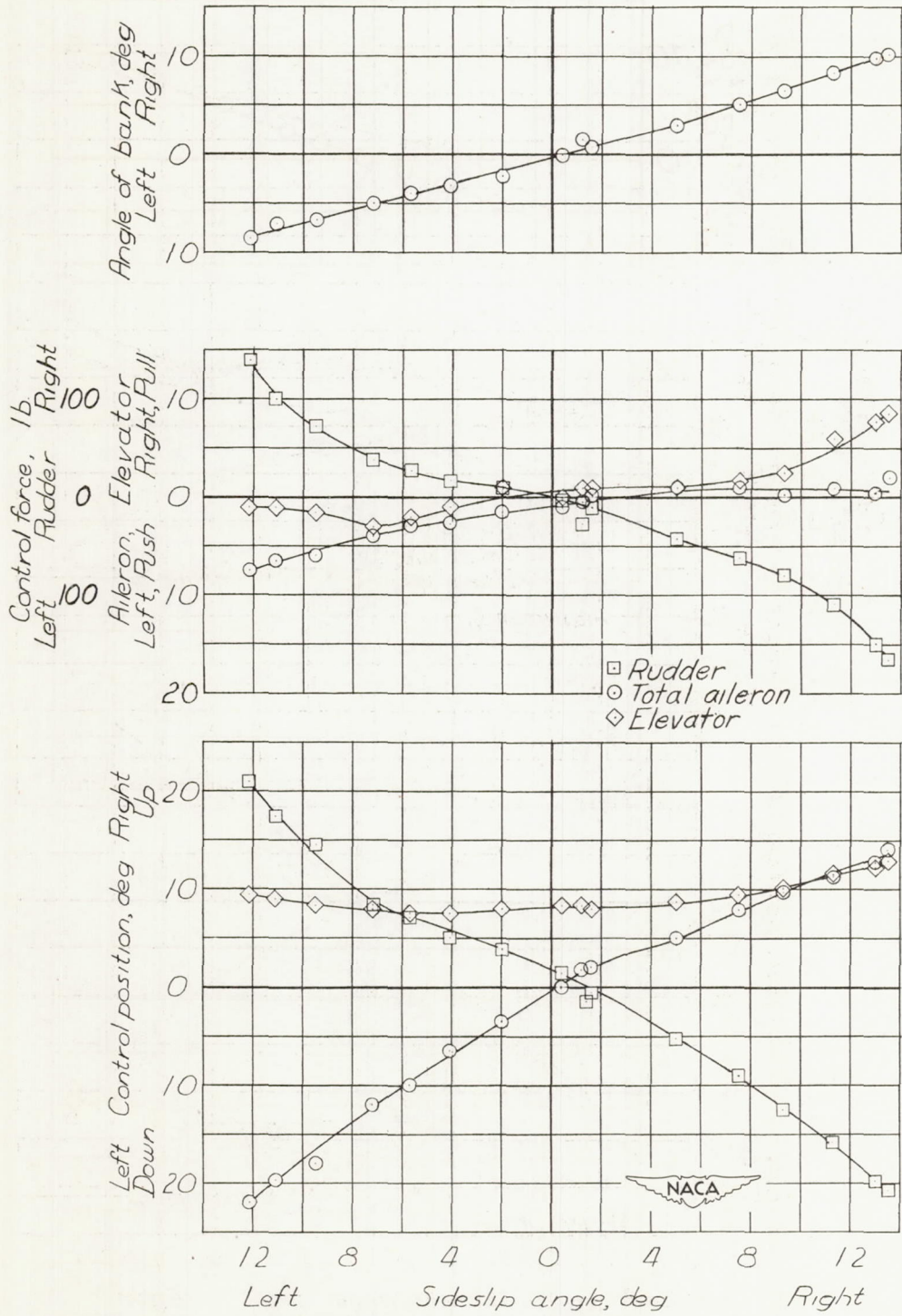
(c) V_c = 135 miles per hour; C_N = 0.74.

Figure 7.- Continued.
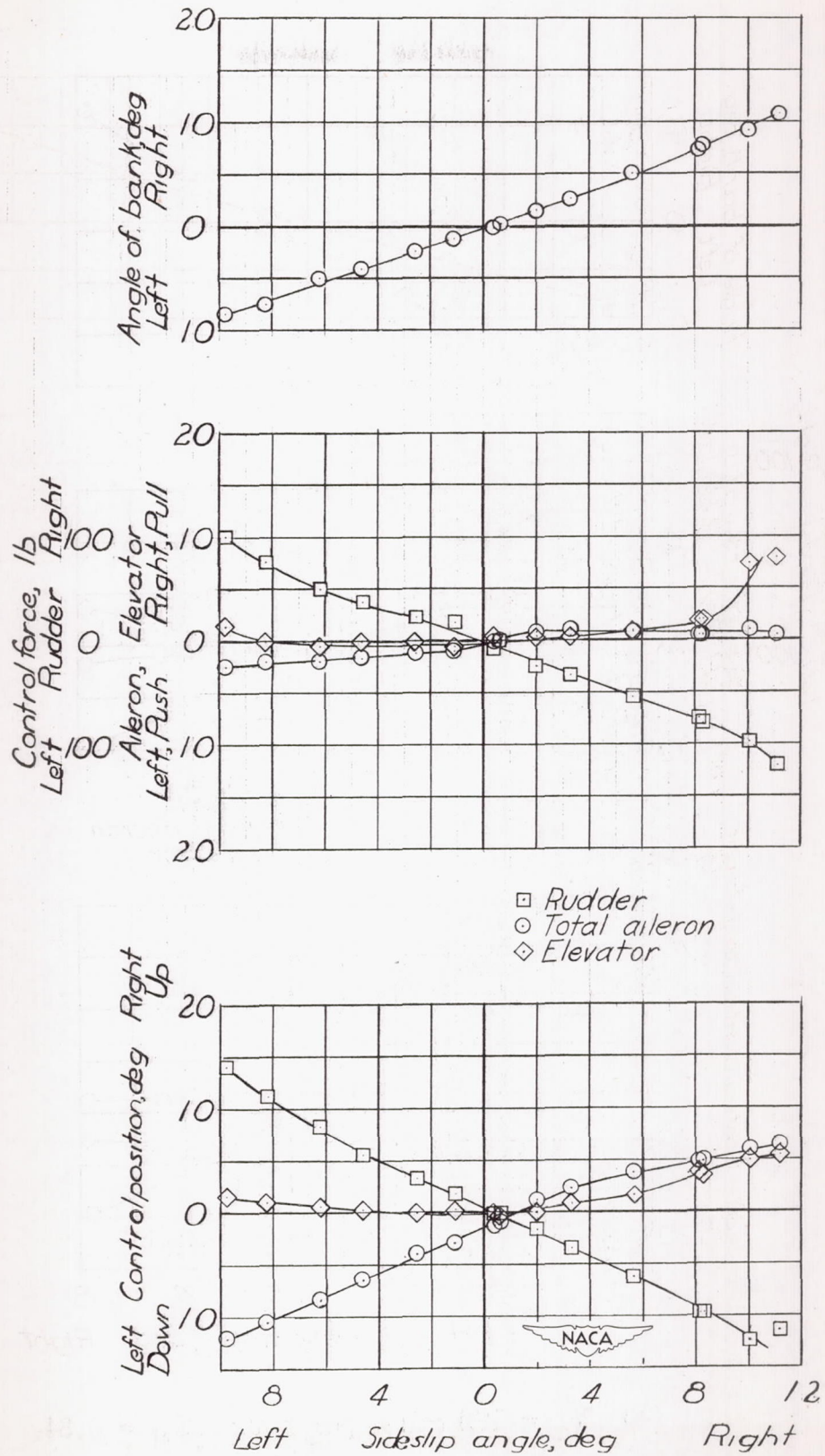
(d) $V_c = 158$ miles per hour; $C_N = 0.54$.

Figure 7.- Continued.
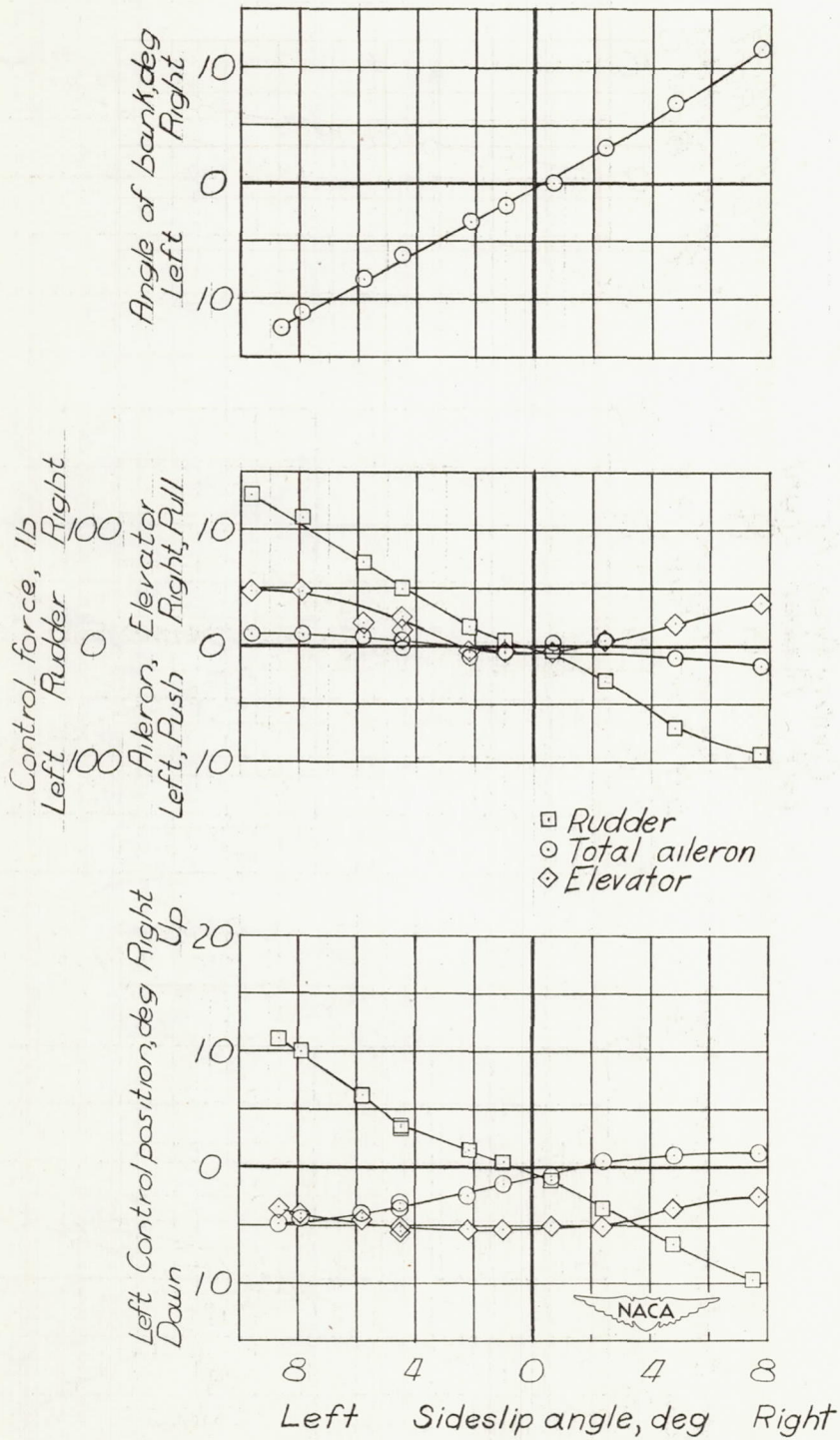
(e) V_c = 198 miles per hour; C_N = 0.34.

Figure 7.- Concluded.
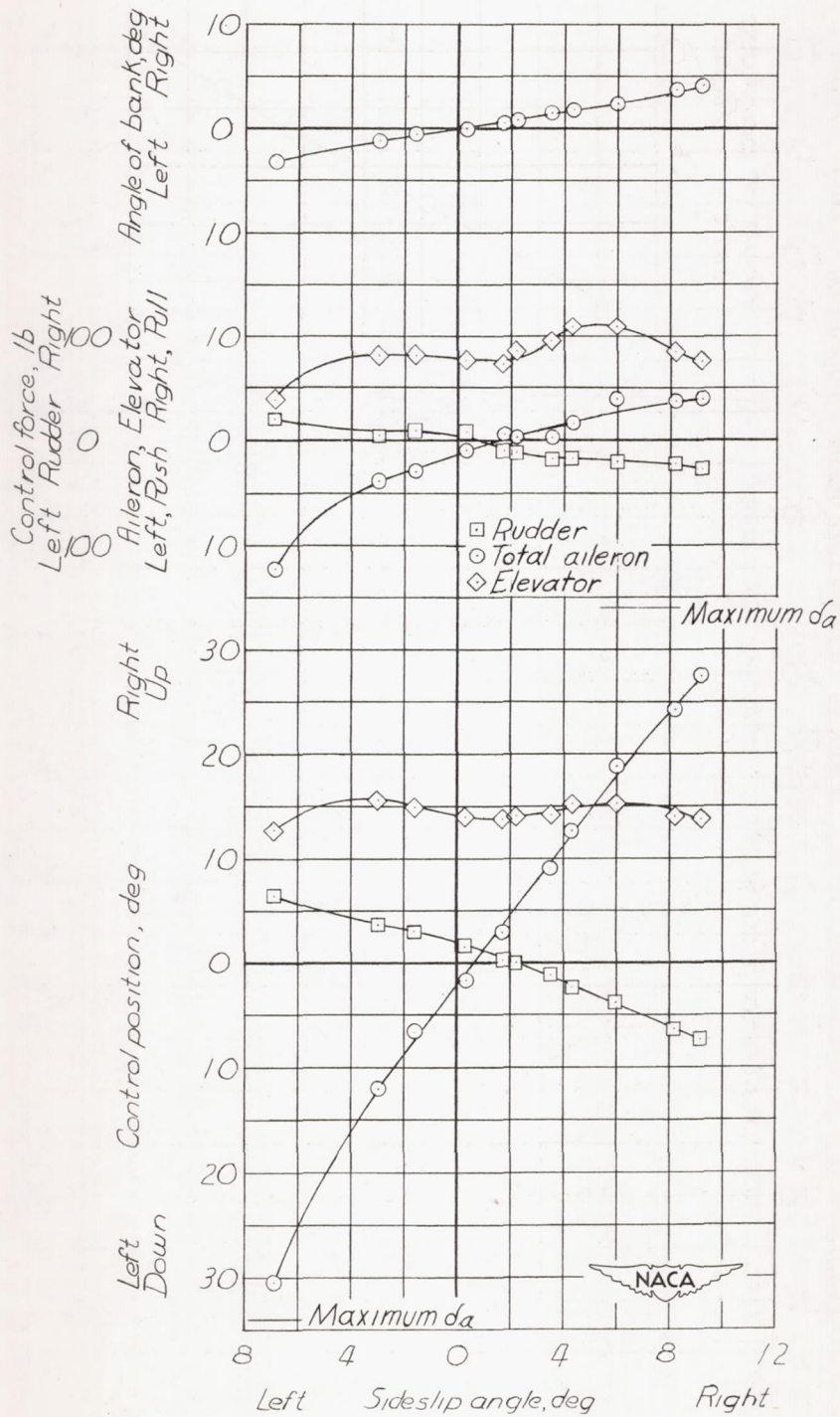
(a) V_c = 111 miles per hour; C_N = 1.10.

Figure 8.- Steady sideslip characteristics with engine idling, flaps down, nose wheel down.
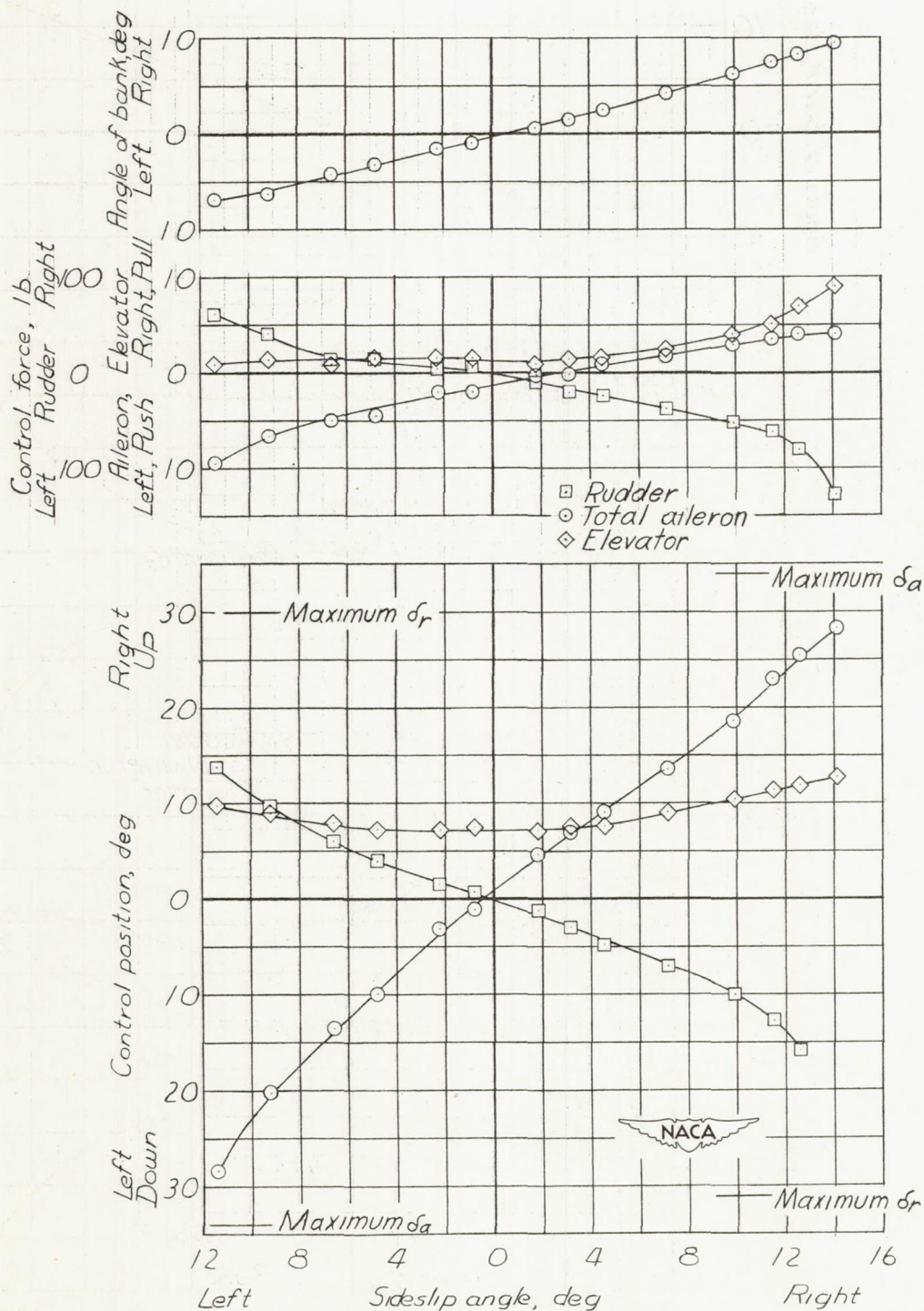
(b) V_c = 131 miles per hour; C_N = 0.78.

Figure 8.- Continued.
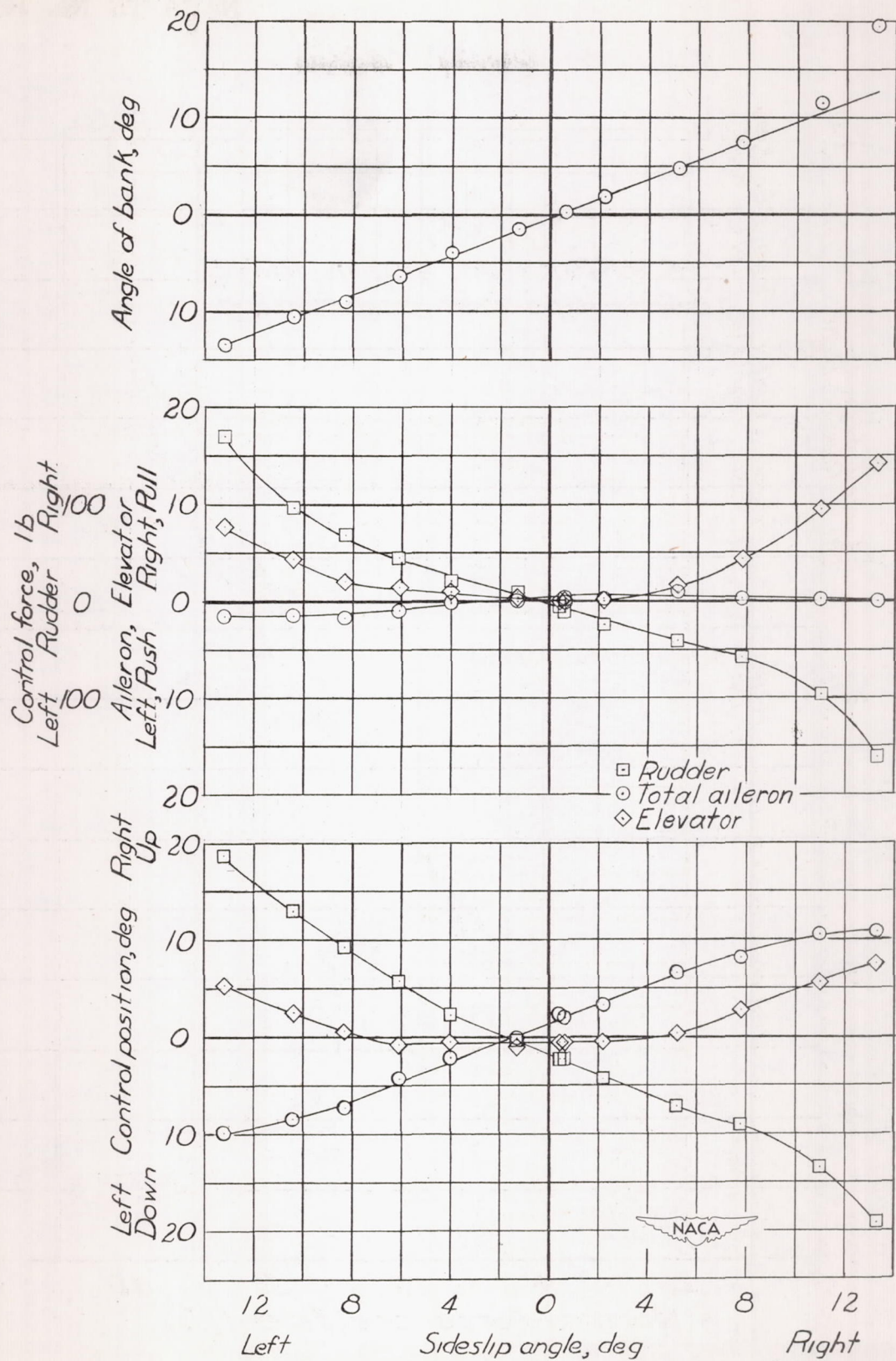
(c) V_c = 159 miles per hour; C_N = 0.53.

Figure 8.- Concluded.
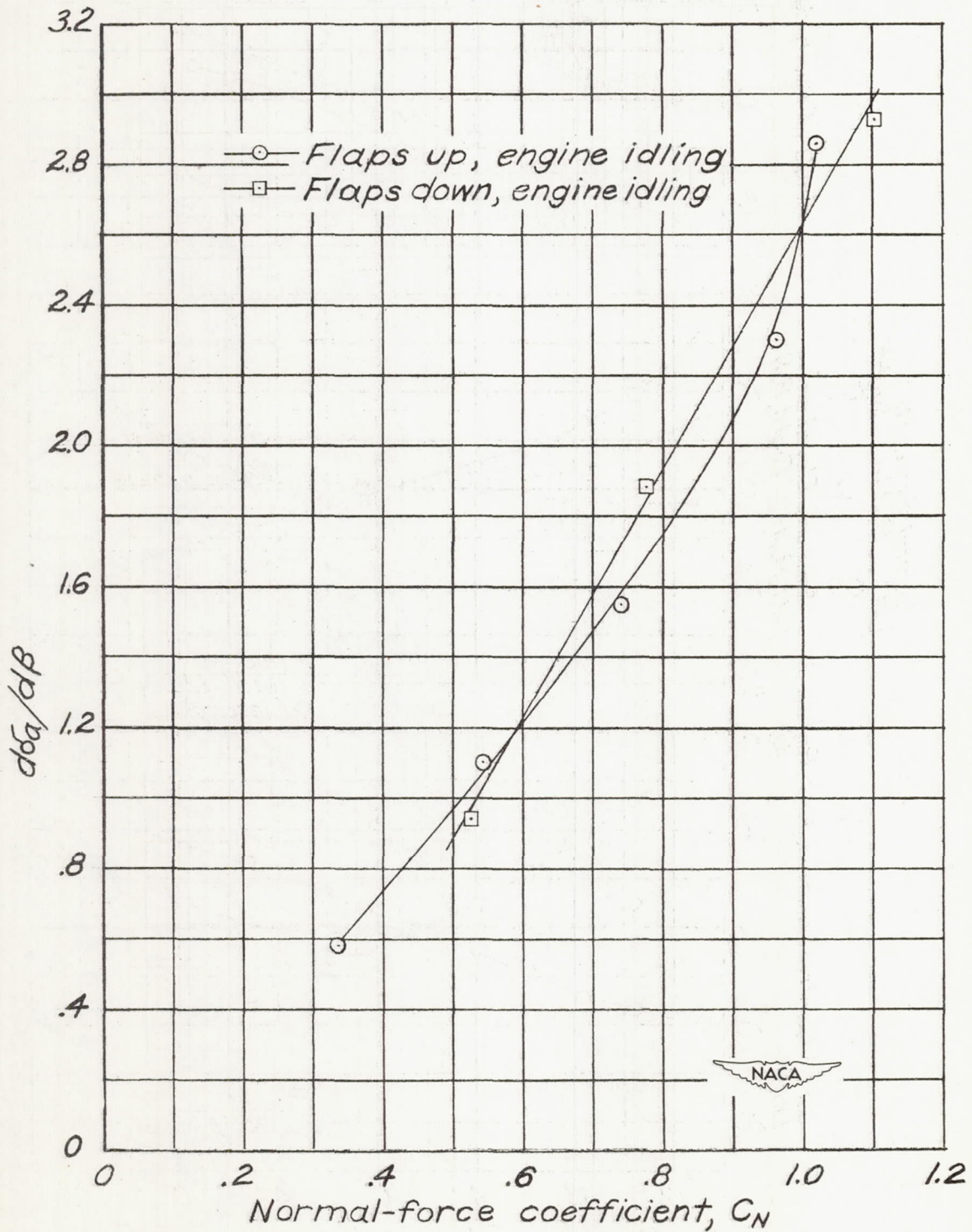
Figure 9.- Variation of $d\delta_a/d\beta$ with C_N as measured in steady sideslips.
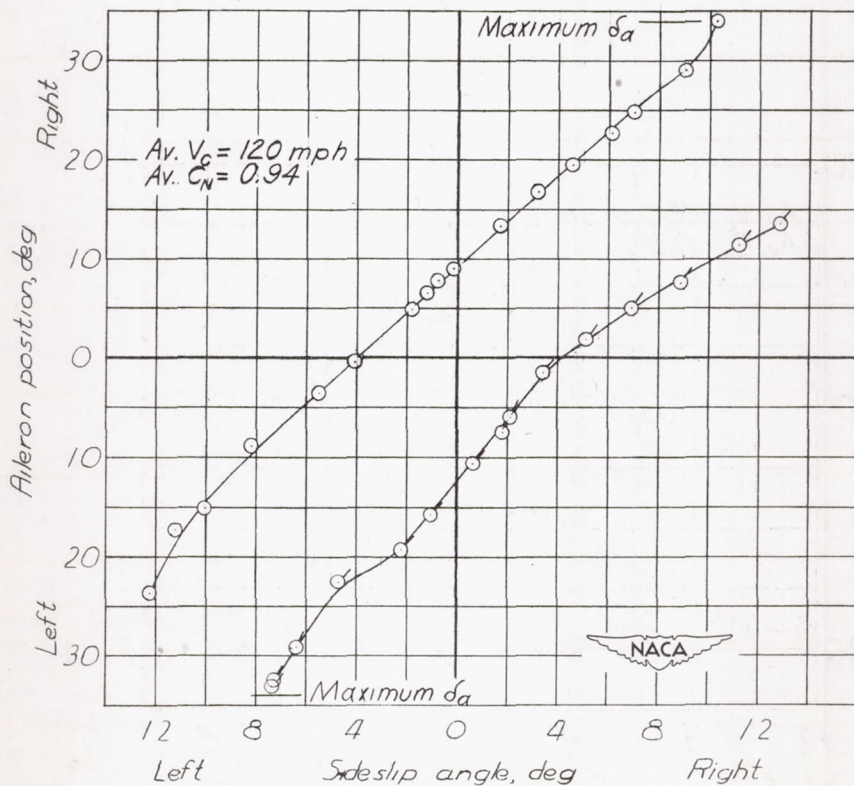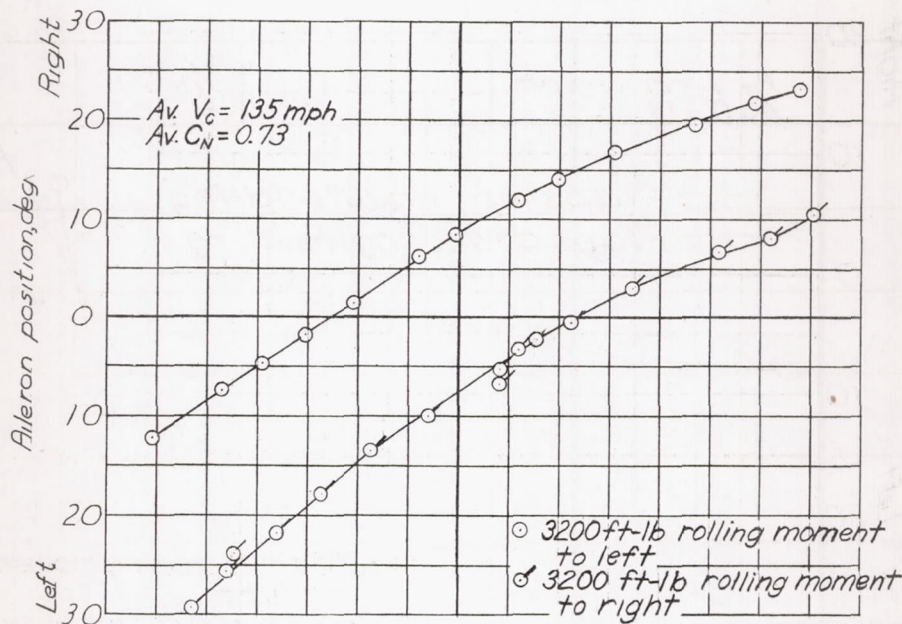
(a) $C_N = 0.94$ and $C_N = 0.73$.

Figure 10.- Variation of aileron angle with sideslip angle in steady
sideslips with airplane asymmetrically loaded. Engine idling;
flaps up; nose wheel up.
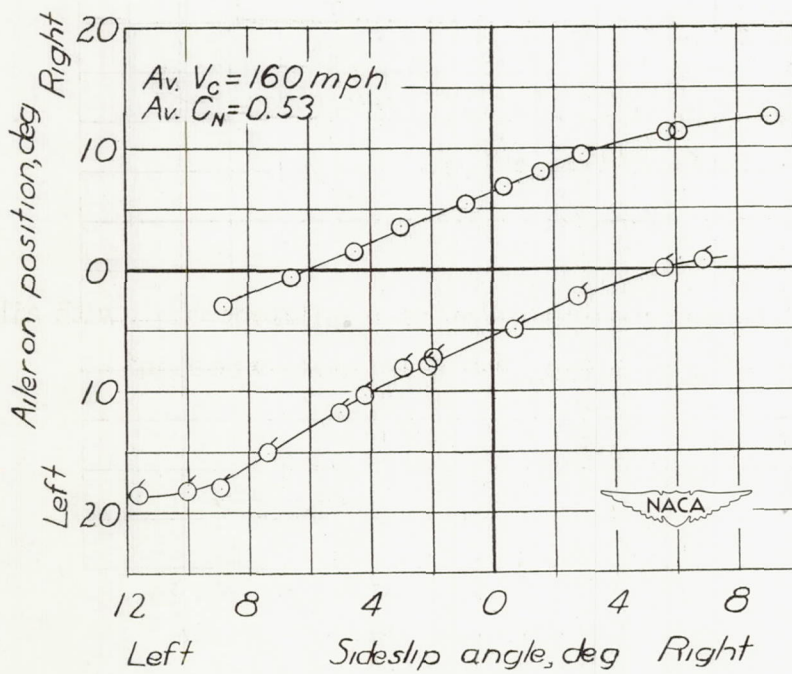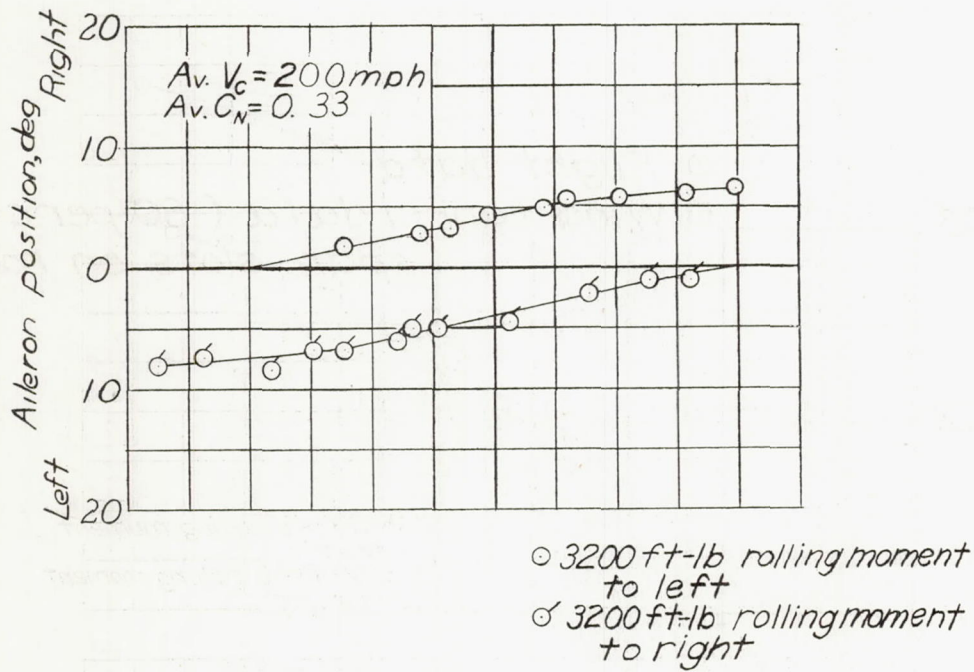
(b) $C_N = 0.53$ and $C_N = 0.33$.

Figure 10.- Concluded.
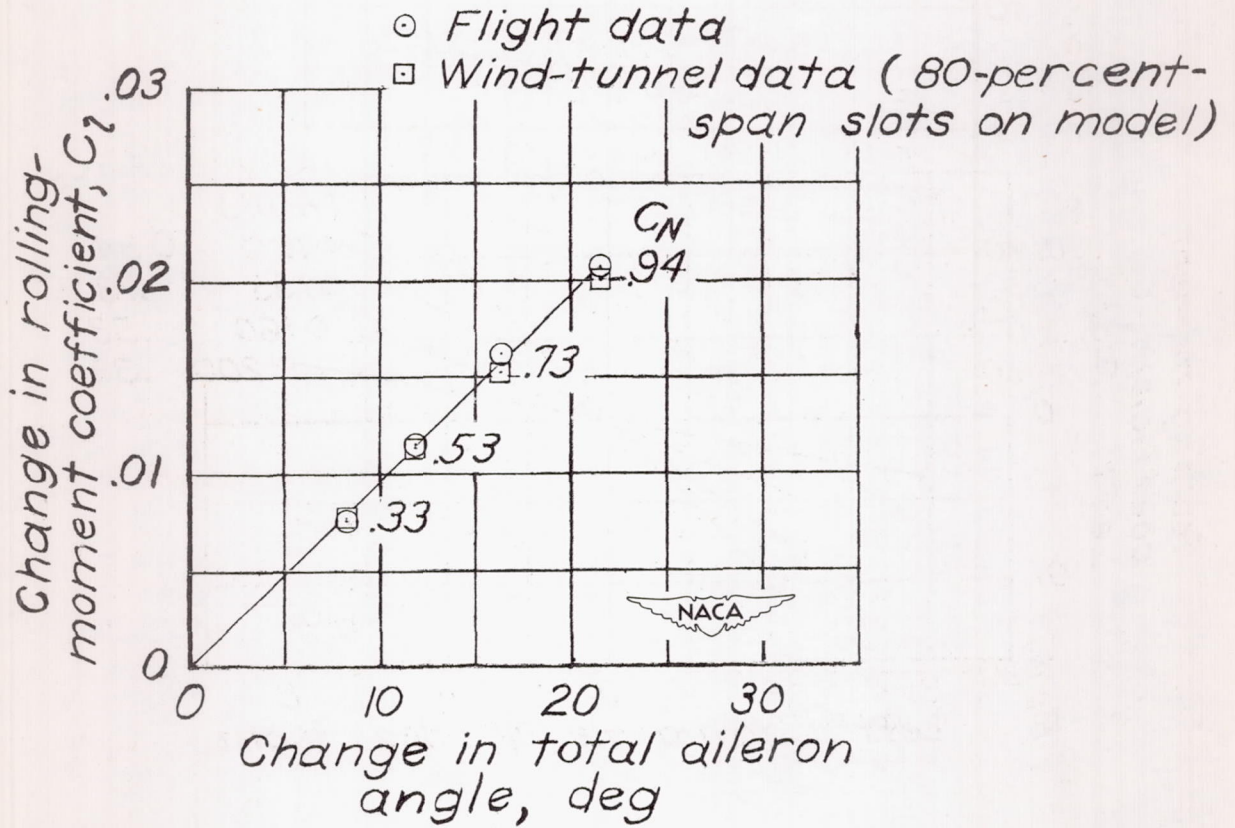
Figure 11.- Variation of rolling-moment coefficient C_l with aileron
deflection δ_a. Engine idling; flaps up; nose wheel up.
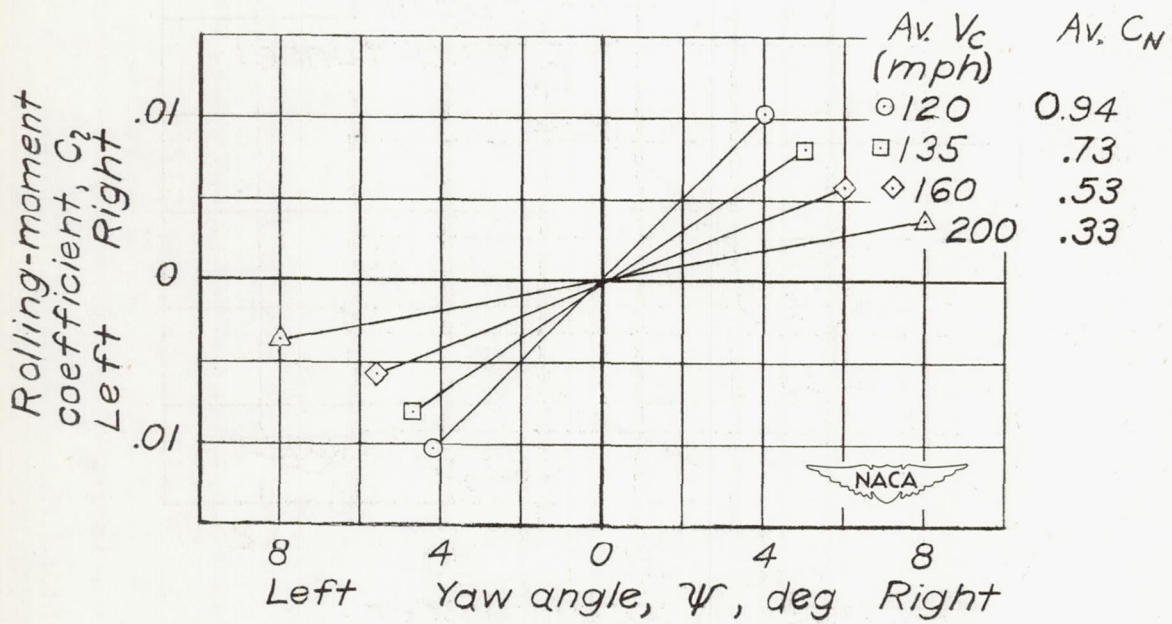
Figure 12.- Variation of rolling-moment coefficient C_l with yaw angle ψ. Engine idling; flaps up; nose wheel up.
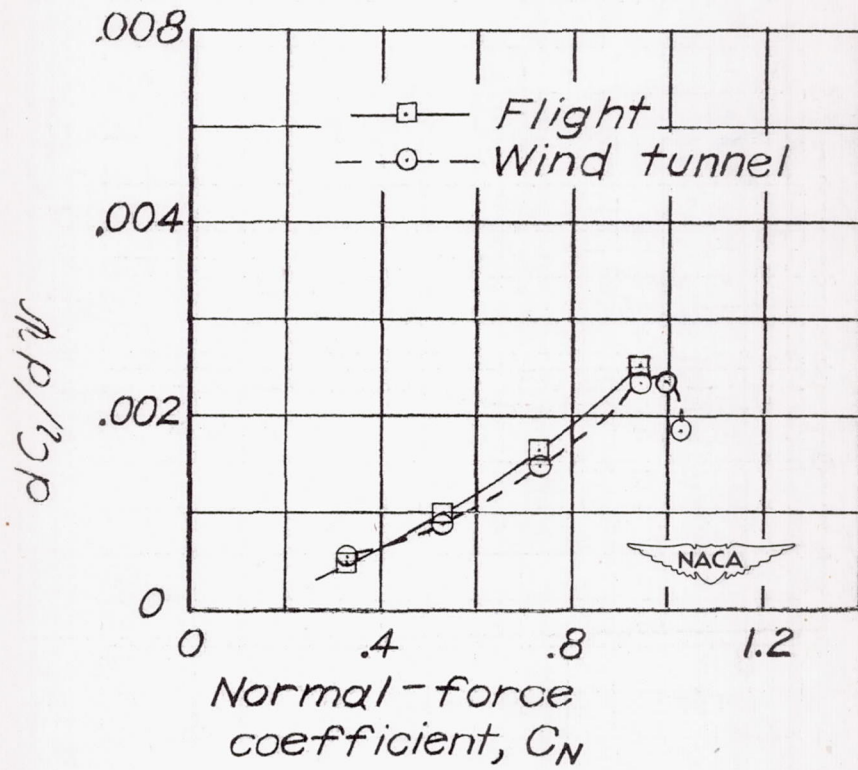
Figure 13.- Comparison of flight and wind-tunnel measurements of dihedral effect. Engine idling; flaps up; nose wheel up.
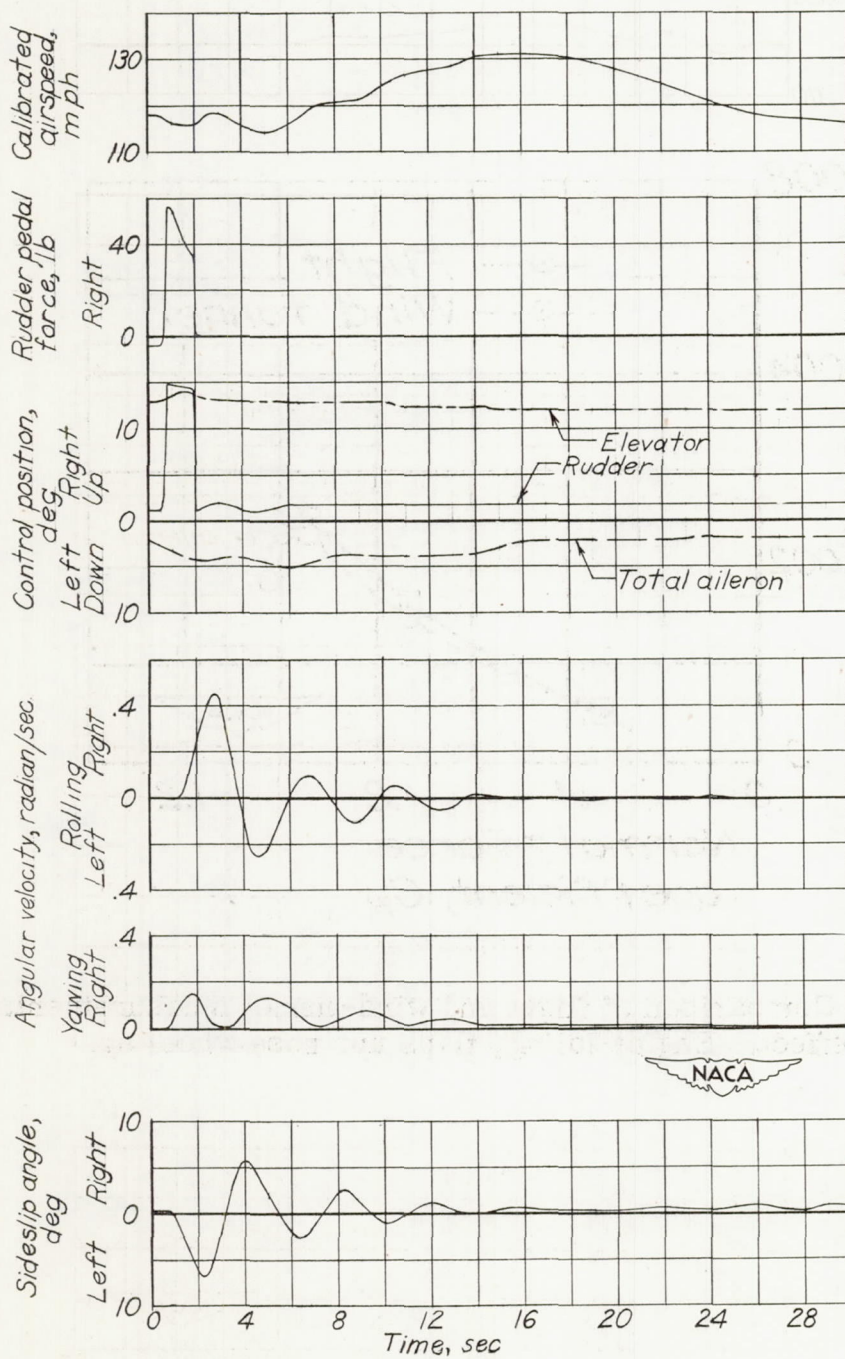
(a) Right rudder deflection.

Figure 14.- Time history of the oscillation resulting from abrupt
deflection and release of the rudder. Pilot attempted to hold control
stick fixed; engine idling; flaps up; nose wheel up; V_c = 120 miles
per hour (approximately).
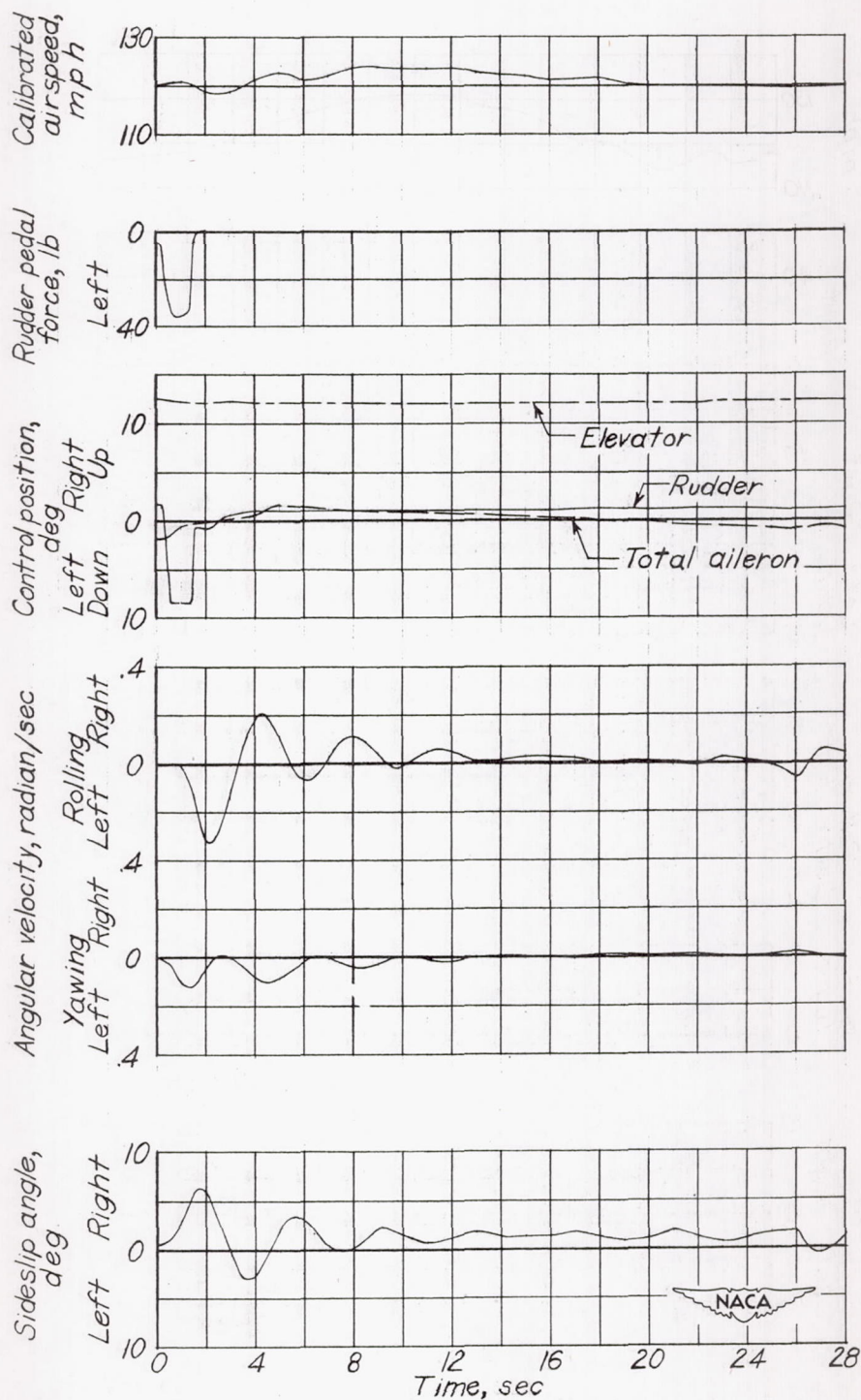
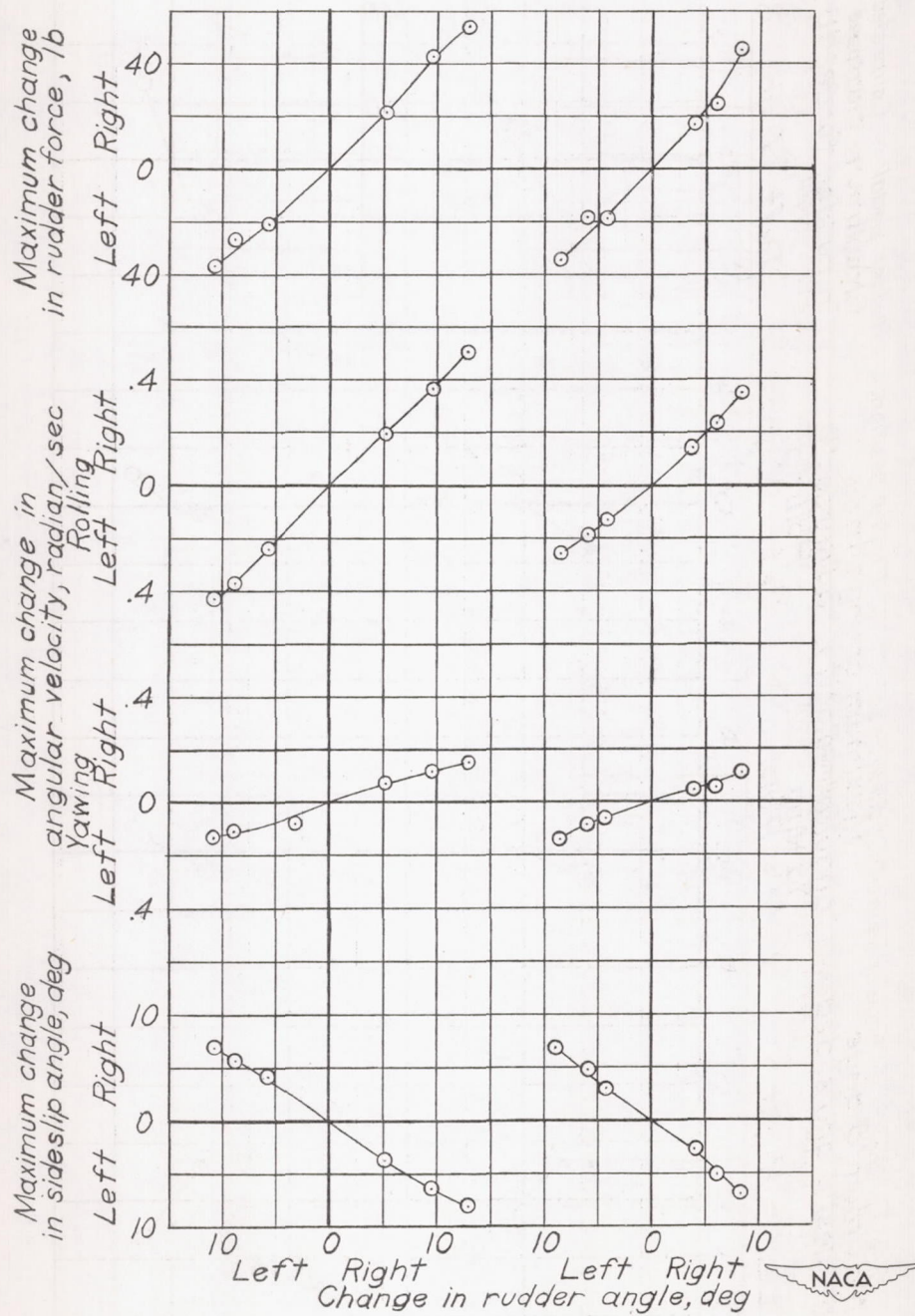(b) Left rudder deflection.

Figure 14.- Concluded.
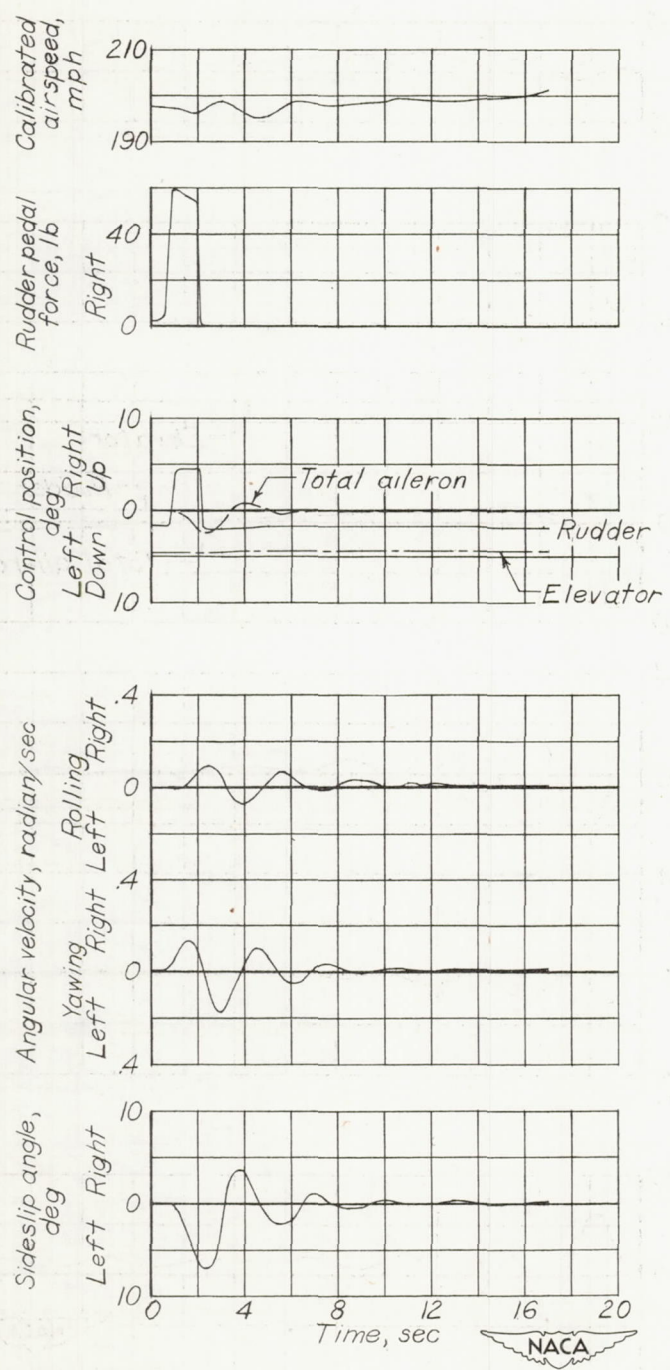
(a) Right rudder deflection.

Figure 15.- Time history of the oscillation resulting from abrupt
    deflection and release of the rudder. Control stick free; engine
    idling; flaps up; nose wheel up; V_c = 200 miles per hour
    (approximately).

(b) Left rudder deflection.

Figuré 15.- Concluded.
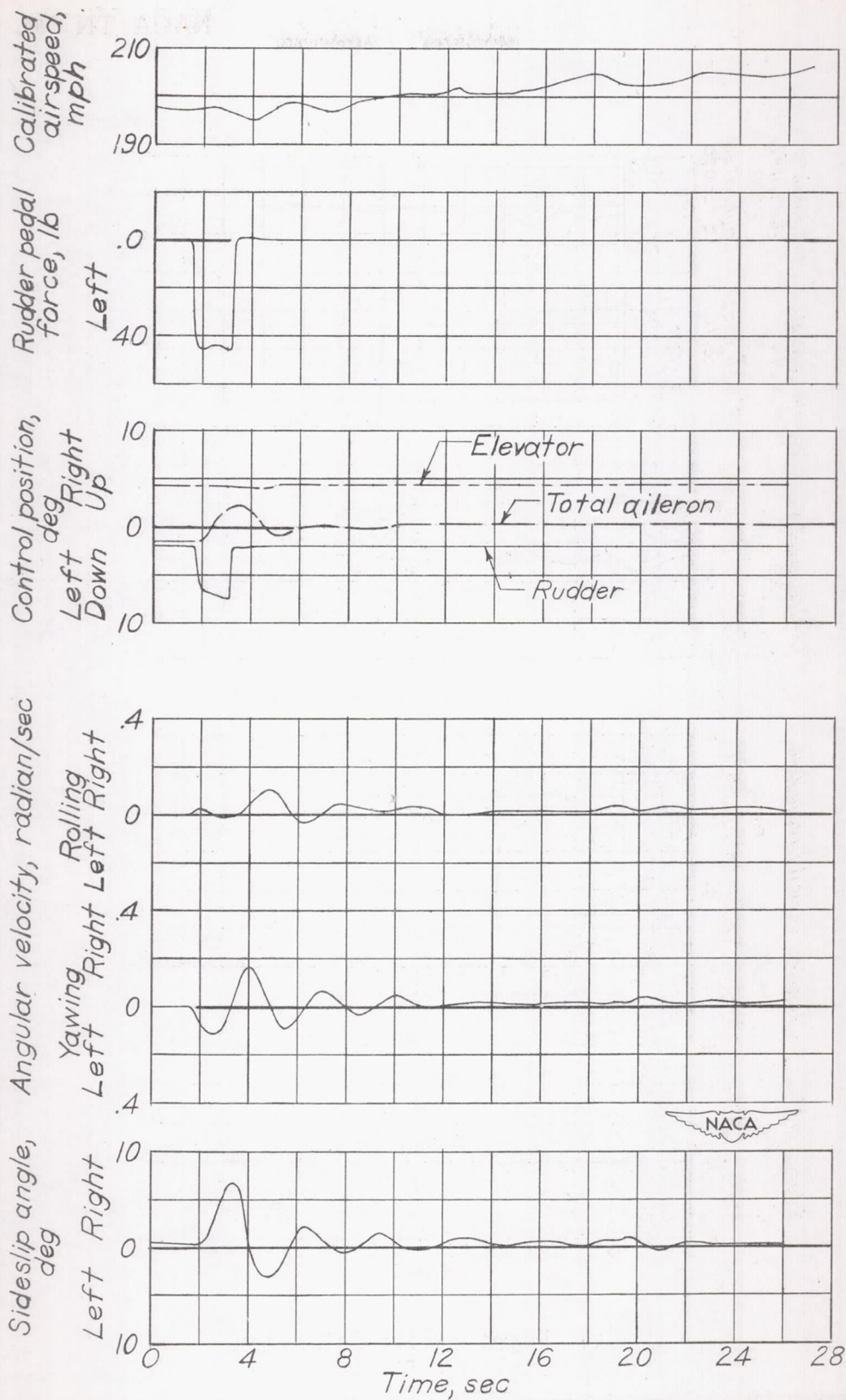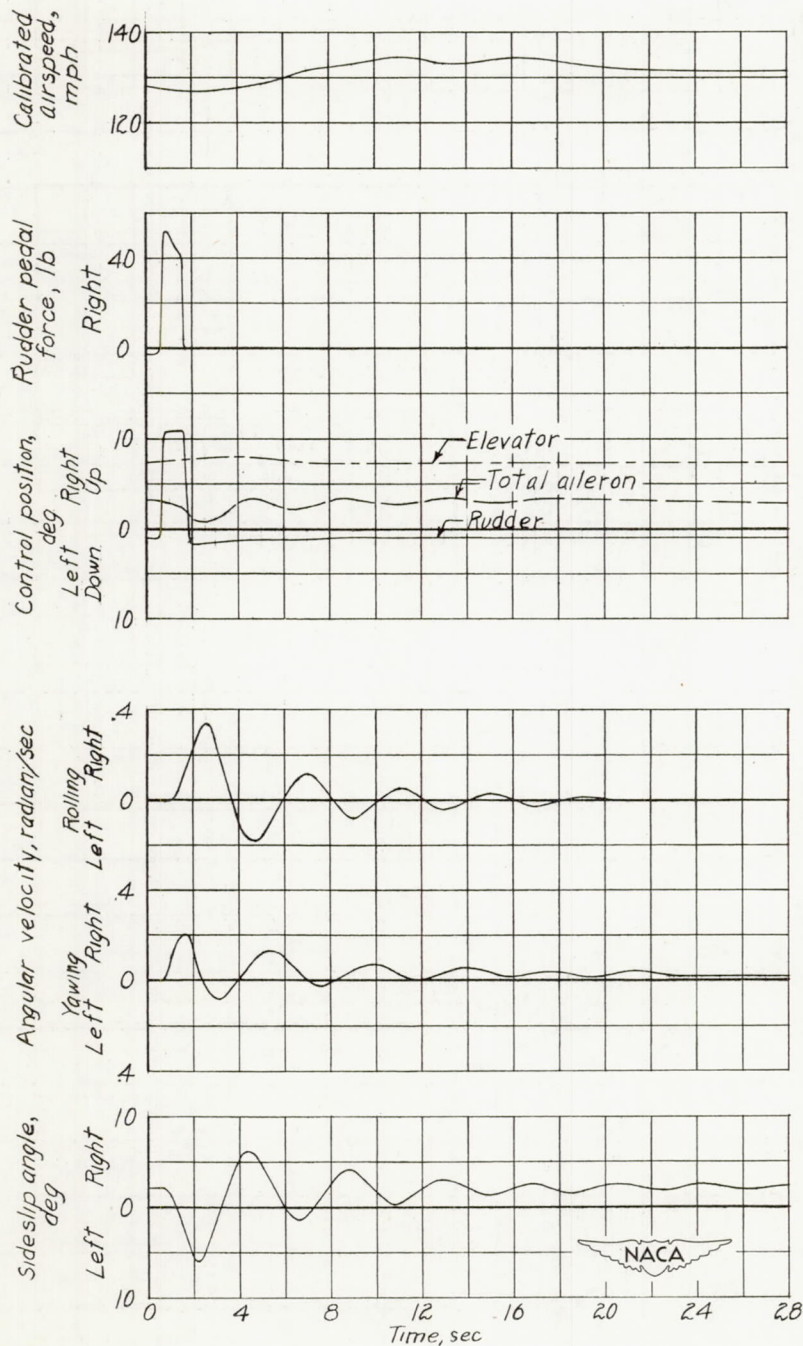
(a) Right rudder deflection.

Figure 16.- Time history of the oscillation resulting from abrupt
deflection and release of the rudder. Pilot attempted to hold
elevator fixed while not resisting aileron motion; engine idling;
flaps down; nose wheel down; V_c = 130 miles per hour
(approximately).
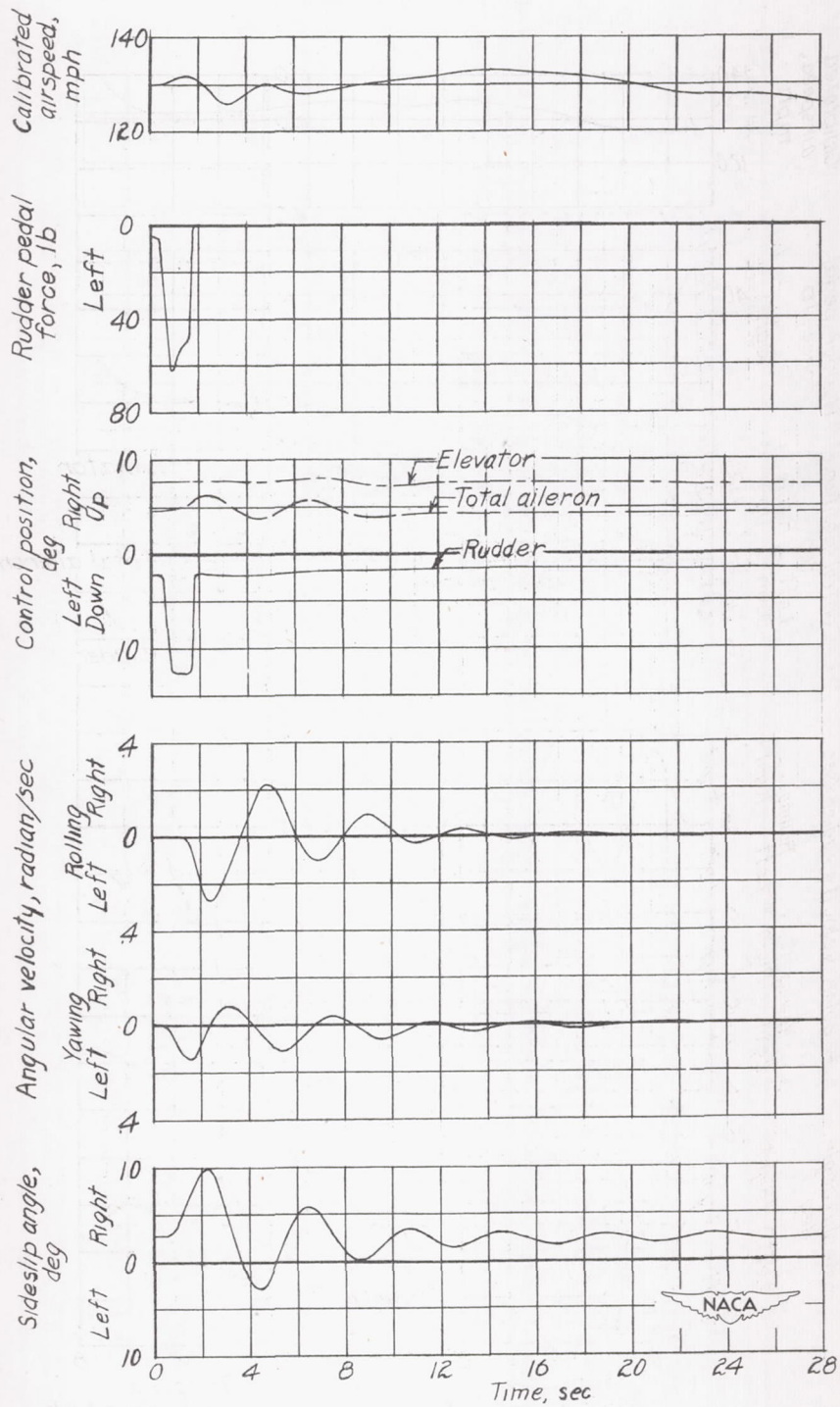
(b) Left rudder deflection.

Figure 16.- Concluded.
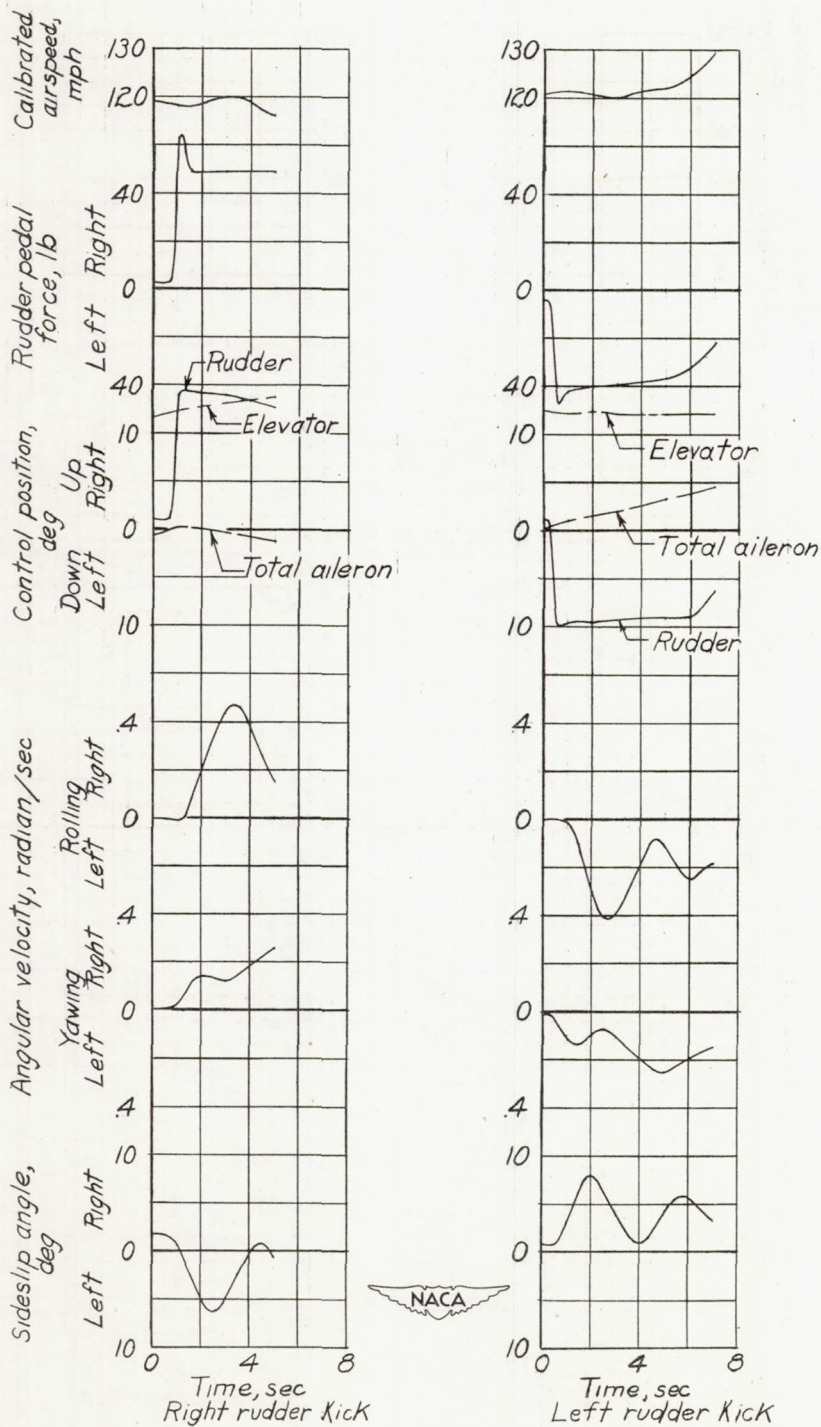
Figure 17.- Time histories of left and right rudder kicks. Pilot
attempted to hold elevator and ailerons fixed; engine idling;
flaps up; nose wheel up; V_c = 120 miles per hour
(approximately).
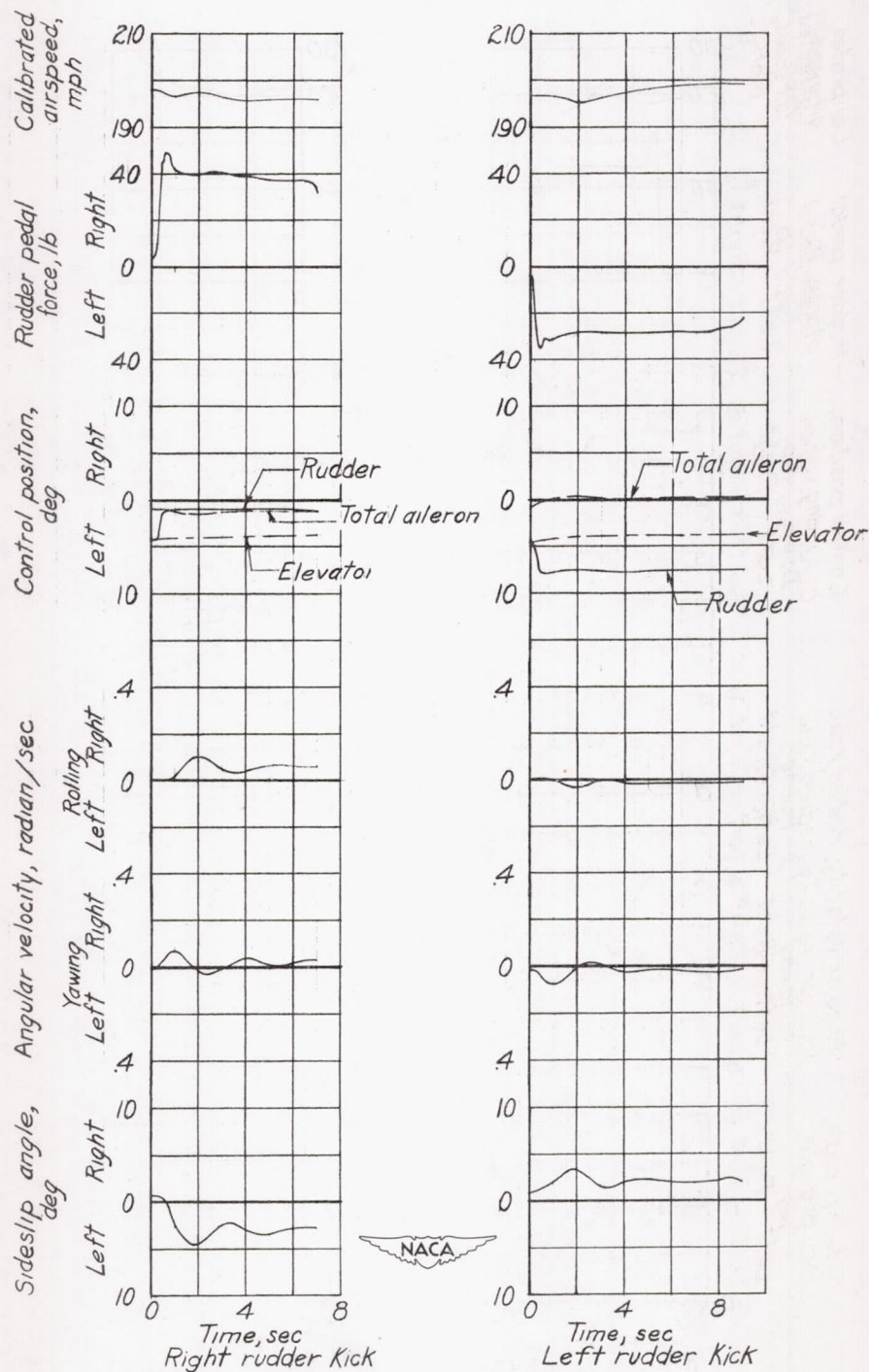
Figure 18.- Time histories of left and right rudder kicks. Pilot
attempted to hold elevator and ailerons fixed; engine idling;
flaps up; nose wheel up; V_c = 198 miles per hour (approximately).
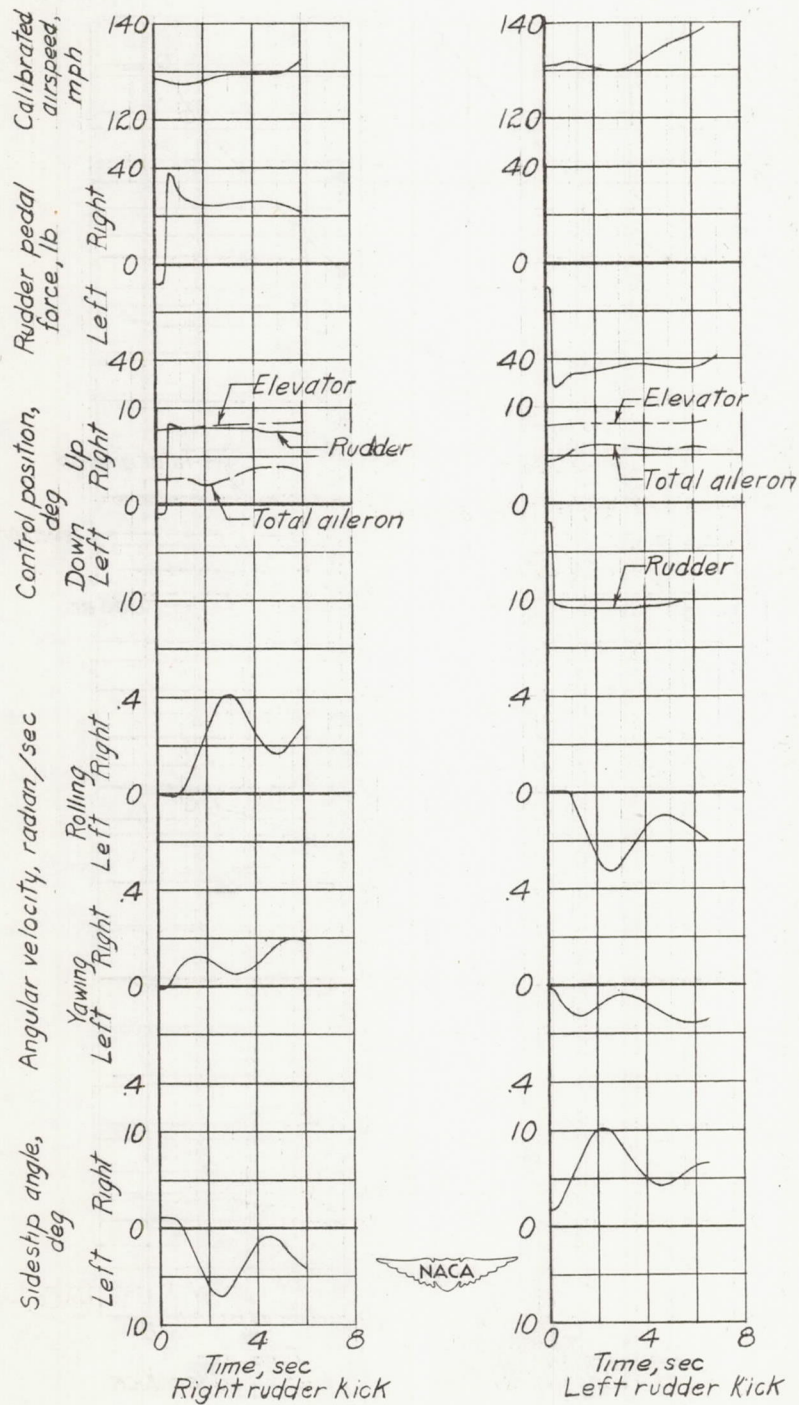
Figure 19.- Time histories of left and right rudder kicks. Pilot
attempted to hold elevator and ailerons fixed; engine idling; flaps
down; nose wheel down; V_c = 130 miles per hour (approximately).
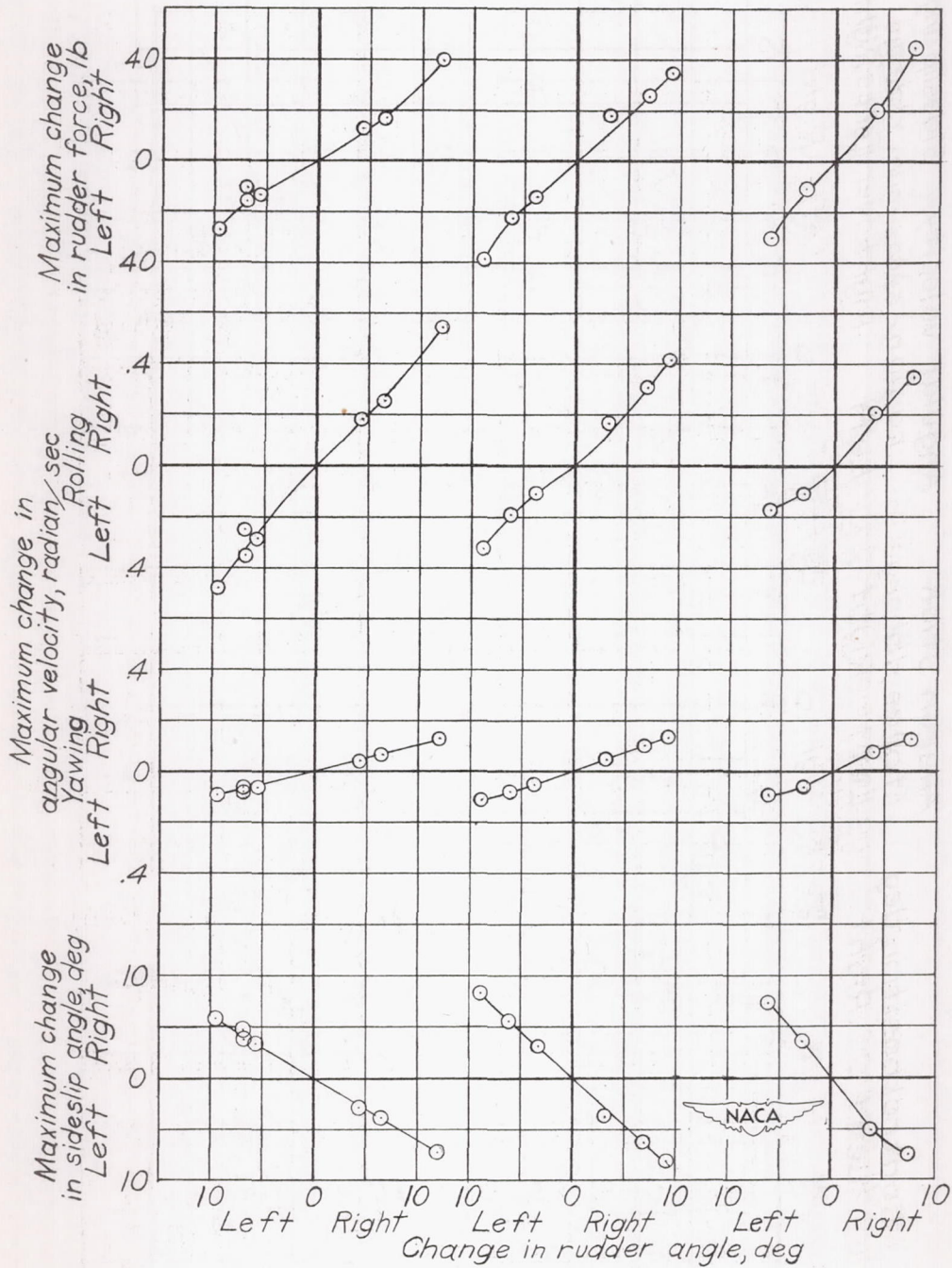
(a) V_c = 120 miles per hour.   (b) V_c = 135 miles per hour.

Figure 20.- Variation of maximum rudder force, rolling velocity, yawing velocity, and sideslip angle with rudder deflection in rudder kicks. Engine idling; flaps up; nose wheel up.
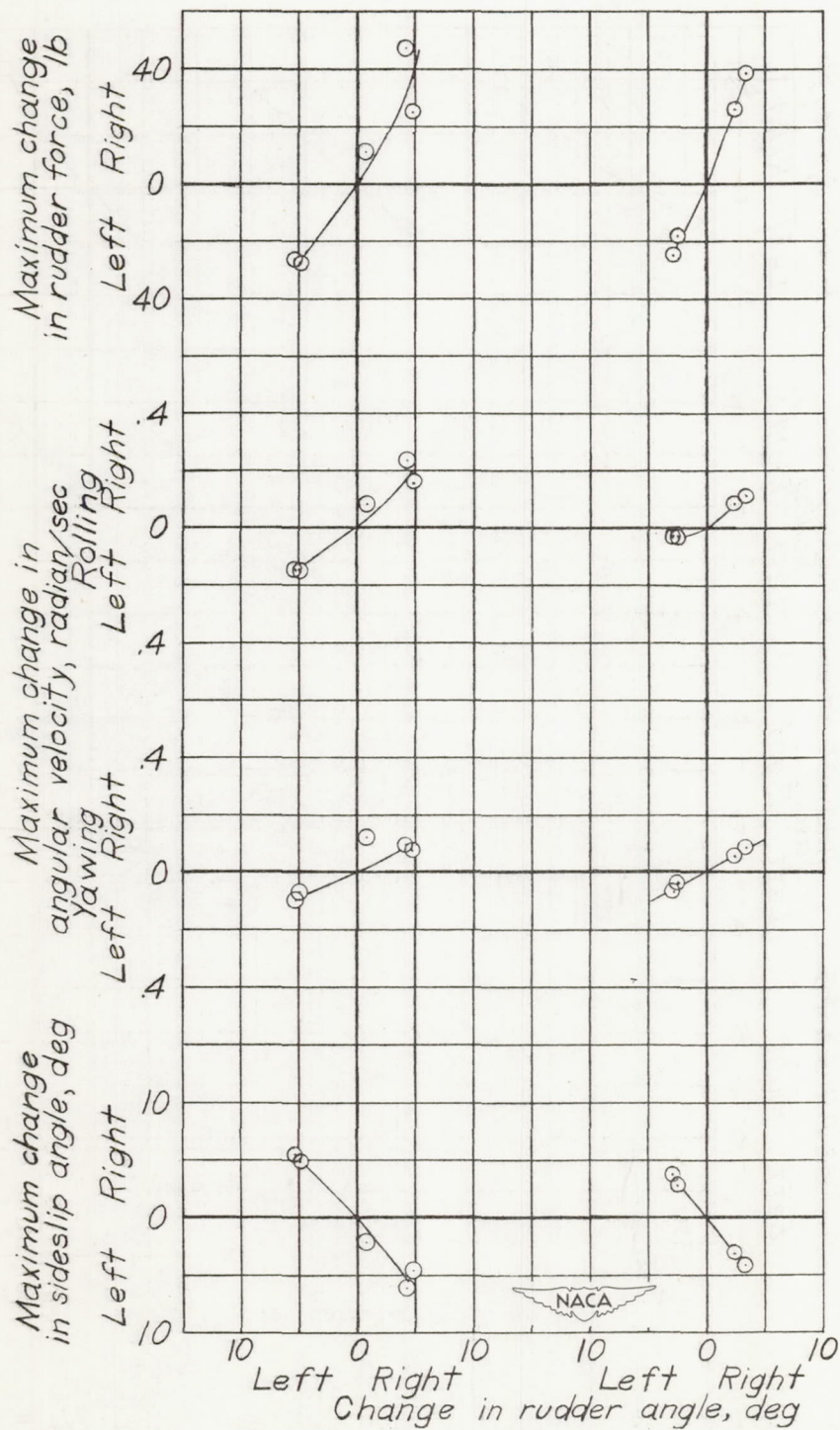
(c) V_c = 160 miles per hour.   (d) V_c = 200 miles per hour.

Figure 20.- Concluded.

(a) V_c = 110 miles   (b) V_c = 130 miles   (c) V_c = 160 miles
per hour.   per hour.   per hour.

Figure 21.- Variation of maximum rudder force, rolling velocity,
yawing velocity, and sideslip angle with rudder deflection in
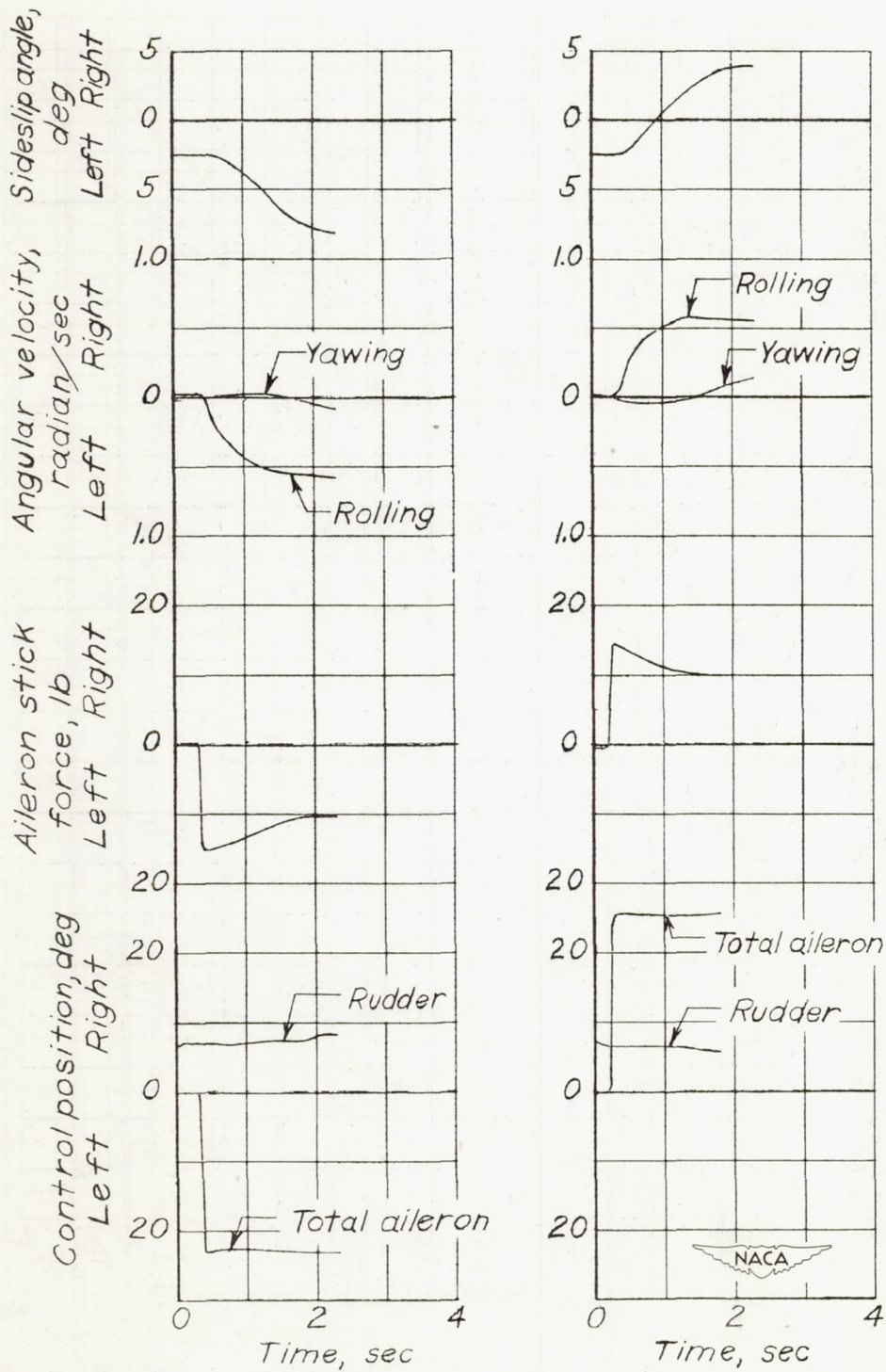rudder kicks. Engine idling; flaps down; nose wheel down.

Figure 22.- Time histories of rudder-fixed left and right aileron rolls.
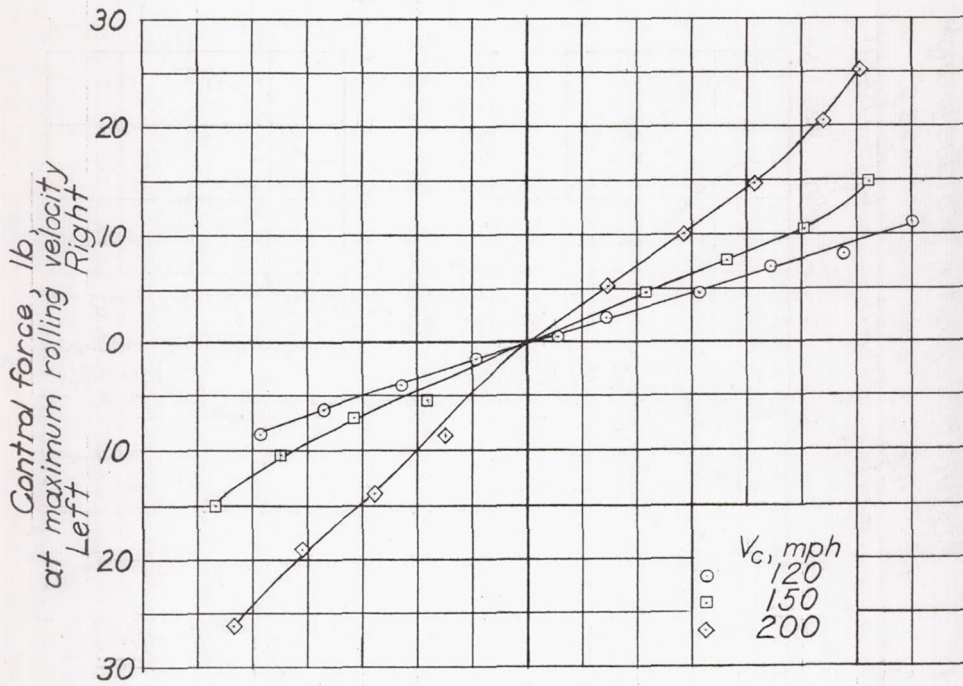Engine idling; flaps up; nose wheel up; V_c = 150 miles per hour.
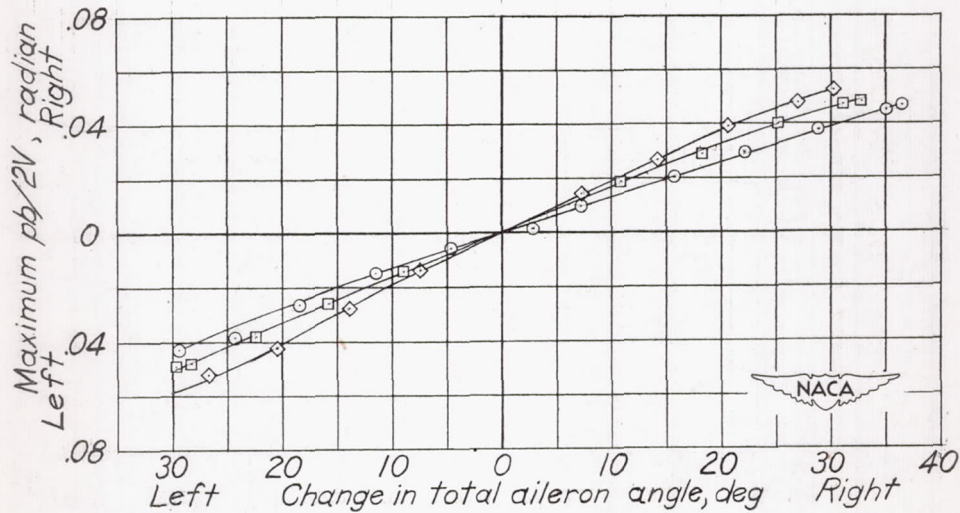
Figure 23.- Variation of aileron stick force and wing-tip helix angle $\frac{pb}{2V}$ with change in total aileron angle in rolls with rudder fixed. Power for level flight; flaps up; nose wheel up.
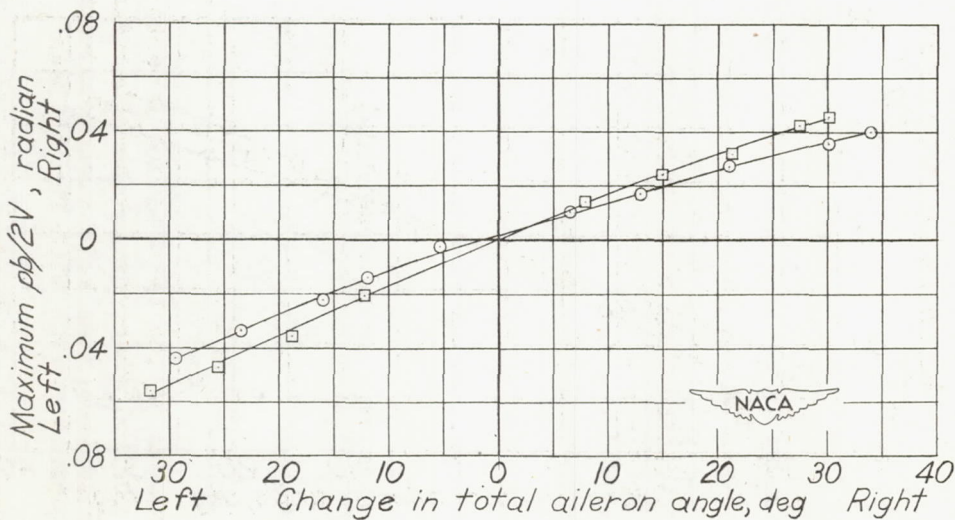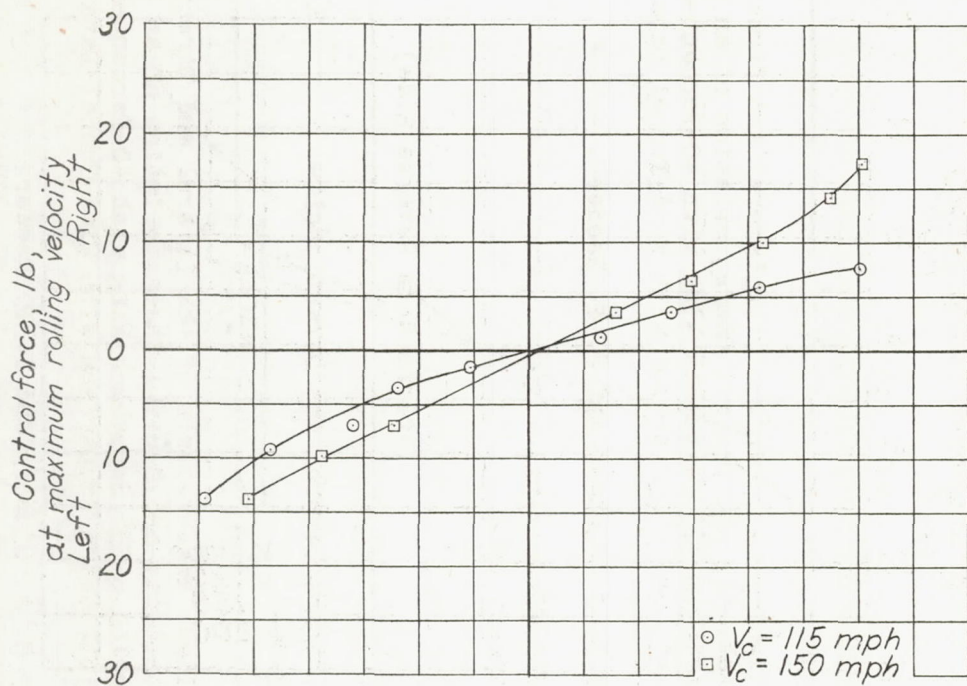
Figure 24.- Variation of aileron stick force and wing-tip helix angle $\dfrac{pb}{2V}$ with change in total aileron angle in rolls with rudder fixed. Power for level flight; flaps down; nose wheel down.